Production and detection of the Higgs bosons of the simplest E_6-based superstring-inspired model

J. F. Gunion and L. Roszkowski*
Department of Physics, University of California, Davis, California 95616

H. E. Haber
Santa Cruz Institute for Particle Physics, University of California, Santa Cruz, California 95064
(Received 21 January 1988)

We explore the phenomenological structure of a string-theory-inspired E_6 grand unified group with low-energy gauge group $SU(2)_L \times U(1)_Y \times U(1)_{Y'}$, with emphasis upon its implications for Higgs-boson production and detection. We first summarize constraints on the theory deriving from known limits on Z-Z' mixing. We then describe how the most general superpotential allowed by E_6 leads to constraints upon and relations among the various Higgs-boson masses, and between the Higgs-boson spectrum, the Z', and the masses of supersymmetric particles. In addition we explore the couplings of the Higgs boson to the gauge and other particles of the theory and emphasize the associated implications for Higgs-boson and supersymmetric-particle detection. The tightly constrained nature of the parameter space of the theory leads to very specific predictions.

I. INTRODUCTION

Although it is likely that superstring theory will lead to many different phenomenologically viable low-energy gauge groups, it is interesting to explore the features of the most attractive case discussed to date. Namely, we consider the simplest E_6-based low-energy group, $SU(2)_L \times U(1)_Y \times U(1)_{Y'}$, resulting from compactification of 10-dimensional $E_8 \times E_8'$ superstring theory to four dimensions on a manifold with a SU(3) holonomy.[1] The resulting theory has many phenomenologically interesting features: it includes a new neutral gauge boson Z'; full $N=1$ low-energy supersymmetry; a number of exotic new fermions; and an extensive Higgs-boson sector. The features of the latter were outlined early on,[2-4] followed by more detailed treatments.[5-9] Here we expand on the work of Ref. 5, focusing on the production and detection of the Higgs bosons of the theory. Related results can be found in Ref. 9. However, the phenomenology of the Higgs bosons is closely tied to the other sectors of the theory and, as a result, we shall also consider Z-Z' mixing, Z' decays, and the mass spectrum of the neutralinos and charginos of the theory.

The compactification scheme of the model predicts that the matter fields occur in three (we adopt the minimal number required) $N=1$ supersymmetric chiral multiplets, each transforming according to the quantum numbers of the fundamental **27** of E_6. Among the fields associated with each such multiplet are five colorless neutral superfields. Of these, one is usually assigned nonzero lepton number. The spin-zero components of the remaining four neutral superfields can potentially acquire nonzero vacuum expectation values as part of the breakdown of the $SU(2)_L \times U(1)_Y \times U(1)_{Y'}$ symmetry. Of these, two belong to doublets of the residual SU(2), and the other two are singlets under SU(2). Within a give **27** multiplet labeled by a ($a=1,2,3$), we denote the two doublet fields by $H_1^{(a)}$ and $H_2^{(a)}$, and the two singlets by $N_1^{(a)}$ and $N_2^{(a)}$. The breaking of the $SU(2)_L \times U(1)_Y \times U(1)_{Y'}$ symmetry down to $U(1)_{EM}$ occurs when some of these "Higgs" fields acquire vacuum expectation values (VEV's). As we shall discuss, it is possible to work in a basis in which the Higgs fields of only one of the three multiplets acquires a nonzero VEV. By convention we define these to be the "third-family" Higgs fields, i.e., only $N_1^{(3)}$, $N_2^{(3)}$, and the neutral components of $H_1^{(3)}$ and $H_2^{(3)}$ can acquire VEV's.

The relation of the third-family defined in this way tc the normal fermions contained in the three **27** E_6 multiplets is more model dependent. In the context of the theory, the symmetry breaking occurs as a result of evolution of one or more of the mass squared terms, appearing in the potential for the above Higgs fields, from a positive value at the grand-unification scale to a negative value at the electroweak scale. The renormalization-group equations that control this evolution imply that a large Yukawa coupling to fermions is required to generate such a negative mass squared in the Higgs potential. Thus, the fermion members of the third-family multiplet defined above should also be those having the largest Yukawa couplings. In other words, the third-family Higgs fields are, by definition, the first (and only) ones to acquire vacuum expectation values and participate in the electroweak symmetry breaking, and the fermions belonging to the same matter multiplet should have the largest Yukawa couplings to these Higgs bosons. An additional argument for this point of view is based on the requirement that flavor-changing neutral currents (FCNC's) are adequately suppressed. To achieve this suppression of FCNC's one must assume that only one of the three generations of Higgs boson couples significantly to the standard-model quarks and leptons.[10]

As usual, several of the degrees of freedom of these third-family Higgs bosons that acquire VEV's are eaten by the W, Z, and Z' in acquiring mass, leaving a certain number of physical Higgs-boson states. The phenome-

nology of these (third-family) Higgs bosons has close similarities to that of the Higgs sector in the minimal supersymmetric model explored in Refs. 11 and 12. They will have trilinear tree-level couplings to vector-boson pairs and their Yukawa couplings to fermions of all generations will be tied to the fermion masses (since only those Higgs fields which acquire vacuum expectation values can produce masses for the fermions). Indeed, many features of their interactions and decays will be analogous to those of the standard-model (SM) Higgs boson. It is these Higgs bosons which will be the focus of the paper. Altogether, their phenomenology is controlled by only five parameters: these can be taken as the mass of the Z', the ratio of the vacuum expectation values of the neutral components of the doublet fields $H_2^{(3)}$ and $H_1^{(3)}$, the masses of two of the physical Higgs bosons, and the scale of gaugino masses (as set by the gluino mass). As a result, relatively well-defined predictions for third-family Higgs-boson production and decay emerge.

In contrast, the Higgs fields of the first and second families by definition do not have vacuum expectation values; we shall follow the nomenclature of Ref. 7 by referring to such scalar fields (with no VEV's) as "unhiggs" bosons. They possess only quartic couplings to vector-boson pairs, and their Yukawa couplings to fermions of their own and other generations cannot be very large. (Since, by definition, the unhiggs fields do not acquire VEV's the latter couplings should be substantially smaller than the Yukawa couplings of the third-generation Higgs bosons to the heavier third-generation fermions.) If the Yukawa couplings are weak, then they will be mainly pair produced via Drell-Yan-type processes. The unhiggs bosons might be relatively light,[7] but in the case of the charged unhiggs bosons they cannot be lighter than the experimental bounds coming from the SLAC and DESY e^+e^- storage rings PEP and PETRA.[13] We will have relatively little to say about these unhiggs bosons.

The plan of the paper is as follows. In Sec. II we give additional details concerning the theoretical structure of the (third-family) Higgs sector and give results for their masses. In Sec. III we consider the neutralinos and charginos of the third family, which are the ones that will be important in Higgs-boson decays. In particular, we present their mass spectrum, which is closely tied to that of the Higgs bosons once the gluino mass is specified. In Sec. IV we discuss couplings of the Higgs bosons to vector-boson pairs and to fermion pairs. These couplings are then used in Sec. V to predict the production phenomenology for the Higgs bosons. In Sec. VI and the Appendix we survey the remaining Higgs-boson couplings that, along with those considered in Sec. IV, control the Higgs-boson decays. These decays are discussed in Sec. VII. Finally, in Sec. VIII we summarize our results and present conclusions.

II. THEORETICAL PRELIMINARIES, CONSTRAINTS, AND THE HIGGS-BOSON MASS SPECTRUM

As reviewed in the Introduction, it is possible to define the Higgs bosons in such a way that only the Higgs bosons associated with the third-generation **27** multiplet of E_6 participate in the electroweak symmetry breaking. Generally there is mixing with the Higgs fields of the other generations at the superpotential level through trilinear couplings that have a matrix form, $\lambda_{abc}H_1^{(a)}H_2^{(b)}N_1^{(c)}$, where $a,b,c=1,2,3$ are generation indices. Considerable simplification occurs if we make a particular choice for the Planck scale supersymmetry-breaking parameters. Recall that we work in a basis for the Higgs superfields in which only third-generation Higgs scalars acquire nonzero vacuum expectation values. It was demonstrated in Ref. 7 that a technically natural choice of parameters exists in which $\lambda_{i33}=\lambda_{3j3}=\lambda_{33k}=0$ for $i,j,k=1,2$. With this convention the masses of the true Higgs bosons can be determined by considering only the portion of the scalar field potential that contains the third-generation Higgs fields. It is to this that we now turn, dropping all reference to the third-family index; in particular, the λ appearing below is λ_{333}.

Focusing on third-family fields only, we note that the quantum numbers of N_1 and N_2 are the same under the residual low-energy symmetry group, $SU(2)_L \times U(1)_Y \times U(1)_{Y'}$, but are different under the larger E_6. As a result, in our notation (described more fully in Ref. 6), only N_1 can couple to the H_1 and H_2, via a term of the form $W=\lambda H_1 H_2 N_1$ in the superpotential. Other possible terms, such as $H_1H_2N_2$ and $m_{N_{12}}^2(N_1^\dagger N_2+\text{H.c.})$, are omitted since they would not be allowed by the underlying E_6 gauge symmetry. The resulting scalar Higgs potential,

$$
\begin{aligned}
V=&\,m_1^2H_1^\dagger H_1+m_2^2H_2^\dagger H_2+m_{N_1}^2N_1^\dagger N_1+m_{N_2}^2N_2^\dagger N_2-\lambda A(H_1H_2N_1+\text{H.c.})\\
&+\lambda^2(H_1^\dagger H_1H_2^\dagger H_2+H_1^\dagger H_1N_1^\dagger N_1+H_2^\dagger H_2N_1^\dagger N_1)+\tfrac{1}{8}(g^2+g'^2)(H_1^\dagger H_1-H_2^\dagger H_2)^2\\
&+\tfrac{1}{72}g_1^2(H_1^\dagger H_1+4H_2^\dagger H_2-5N_1^\dagger N_1-5N_2^\dagger N_2)^2+(\tfrac{1}{2}g^2-\lambda^2)\,|\,H_1^\dagger H_2\,|^2\,,
\end{aligned}
\tag{1}
$$

where g_1 is the $U(1)_{Y'}$ coupling constant, is completely fixed in terms of only two parameters (in addition, to the vacuum expectation values of the Higgs fields described below): λ, defined above; and λA, which specifies the strength of the soft-supersymmetry-breaking scalar potential term, $\lambda A H_1H_2N_1$, appearing above. Other soft supersymmetry-breaking terms in the potential can be eliminated in terms of these two parameters and the

Higgs-field vacuum expectation values by employing the minimization conditions.

The desired minimum of the potential [Eq. (1)] is such that λA is real and positive. By further phase redefinitions, the vacuum expectation values of the neutral fields can also be chosen to be real and positive. Thus, the Higgs potential is *CP* invariant, and the physical scalar Higgs fields derive from the real parts of the neutral components of H_1 and H_2 and the real parts of N_1 and N_2. For simplicity we shall assume that only the first three fields acquire vacuum expectation values—v_1, v_2, and n, respectively. (Our results are not sensitive to this assumption. It has also been argued[14] that a nonzero VEV for N_2 would lead to a variety of phenomenological and theoretical difficulties.) In this case the first three of the above neutral Higgs fields mix to form three physical mass eigenstates, while the real part of N_2 remains an unmixed mass eigenstate, N^0. This last neutral scalar may only be pair produced, and will not play any role in the phenomenology to be discussed; we drop it from consideration. In addition to the three remaining Higgs neutral scalars, there is a single Higgs pseudoscalar, denoted by H_3^0, and a charged Higgs boson $H^{\pm}$. This notation follows the closely related minimal two-doublet supersymmetry model explored in Refs. 11 and 12. (The terms scalar and pseudoscalar refer to the way in which a given neutral Higgs boson couples to a fermion-antifermion pair.)

Let us also fix our notation for the vector-boson sector of the theory. Aside from the charged $W^{\pm}$ and the photon, there are two massive neutral gauge bosons, denoted by Z and Z', with $m_Z < m_{Z'}$. The mixing angle between them is denoted by δ. We fix the gauge coupling constants by $g = e/\sin\theta_W$, $g_1 = g' = g\tan\theta_W$ and $\sin^2\theta_W = 0.23$. [The condition $g_1 \approx g'$ is expected from renormalization-group arguments.[2,3] Here, g_1 is the coupling associated with the $U(1)_{Y'}$ subgroup.] In addition, we take

$$m_W \equiv g(v_1^2+v_2^2)^{1/2}/\sqrt{2} = 83 \text{ GeV} ,$$

and define $m_{Z_{SM}} \equiv m_W/\cos\theta_W$.

With this background it is now possible to specify a convenient independent set of physical parameters for the theory. In addition to m_W, g, g', and g_1, these are $m_{Z'}$, $\tan\beta = v_2/v_1$, $m_{H_3^0}$, and $m_{H^{\pm}}$. Of these, the value of m_W and choices for $m_{Z'}$ and $\tan\beta$ completely determine v_1, v_2, and n. The Z-Z' mixing angle δ, mentioned above, is given by

$$\tan\delta = \frac{g_1 m_W^2 \cos\theta_W (4\tan^2\beta - 1)}{3g(m_{Z'}^2\cos^2\theta_W - m_W^2)(\tan^2\beta+1)} . \tag{2}$$

For future reference, it will also be useful to give an approximate relation between $m_{Z'}$ and n, valid for large n:

$$m_{Z'}^2 = \frac{25}{18}g_1^2 n^2 + \frac{g_1^2}{9g^2} m_W^2(\cos^2\beta + 16\sin^2\beta) + O\left[\frac{1}{n^2}\right] . \tag{3}$$

The experimental constraints on $m_{Z'}$ and δ are outlined in Refs. 15 and 16 and possible future bounds considered in Ref. 17. (The θ_{mix} of this latter reference is related to our mixing angle by $\theta_{\text{mix}} = -\delta$.) However, if $\tan\beta$ is known then the constraints on $m_{Z'}$ and δ are linked, which can significantly reduce the allowed region of parameter space. It is therefore of interest to consider to what extent $\tan\beta$ is predicted in supersymmetric models. In the early days of supergravity model building, a large t-quark Yukawa coupling was used to trigger $SU(2)\times U(1)$ breaking in the low-energy theory.[18] This invariably led to the result that $\tan\beta > 1$. In the many models constructed subsequently, which contained a rather light top quark ($m_t \sim 40$ GeV), $\tan\beta$ tended to be of order 1. In fact, all the superstring-motivated models discussed in the literature seem to have $\tan\beta \gtrsim 1$ (see Refs. 3 and 4, for example). Basically, due to renormalization effects, one finds that at the weak scale, $m_2^2 \ll m_1^2$, which leads to $v_2 > v_1$. One can probably devise schemes to circumvent this conclusion. However, as a heavier top-quark becomes more likely, the tendency to have $\tan\beta > 1$ becomes more difficult to avoid.

A restriction such as $\tan\beta \geq 1$ leads to potentially powerful constraints on $m_{Z'}$ and δ. This is because the ordering $v_2 \gtrsim v_1$ requires relatively large values of δ, especially for small $m_{Z'}$. For instance, the choice

$$\tan\beta \equiv v_2/v_1 = 1.1 \tag{4}$$

yields δ values that do not fall within present neutral-current data bounds unless $m_{Z'} \gtrsim 350$ GeV (Refs. 5 and 19). Probable future bounds, as computed in Ref. 17, would force $m_{Z'} \gtrsim 0.5$ TeV. Significant improvements in any of several experimental measurements involving the Z could easily require large Z' masses in order to maintain $v_2/v_1 \gtrsim 1$. Alternatively, observation of a light Z' in combination with improved Z information could require values of v_2/v_1 that appear difficult to accommodate within the context of the theory.

For the rest of this work we shall adopt the choice (4). The remaining free Lagrangian parameters are λ and λA, mentioned earlier. These are completely fixed (once v_1, v_2, and n have been determined by specifying $m_{Z'}$ and $\tan\beta$) by choosing values for $m_{H^{\pm}}$ and $m_{H_3^0}$:

$$\lambda A = \frac{m_{H_3^0}^2 v_1 v_2 n}{v_1^2 n^2 + v_2^2 n^2 + v_1^2 v_2^2} ,$$
$$\lambda^2 = \frac{m_W^2 - m_{H^{\pm}}^2}{v_1^2+v_2^2} + \frac{n^2 m_{H_3^0}^2}{v_1^2 n^2 + v_2^2 n^2 + v_1^2 v_2^2} . \tag{5}$$

We note that the Higgs-boson mass spectrum and couplings are quite insensitive to the value of v_2/v_1, when considered as functions of $m_{Z'}$, $m_{H_3^0}$ and $m_{H^{\pm}}$. Extreme values of v_2/v_1 (either very large or very small) would be required to significantly alter our results regarding the Higgs sector as presented below. Note also that the sign of λ is not determined in terms of the above two Higgs-boson masses, although the sign of λA is. However, for convenience, we take $\lambda > 0$ for the ensuing discussion in

this section.

We begin by presenting in Fig. 1 the upper and lower bounds for $m_{H^\pm}$, the masses of the heavier two neutral scalars, and the upper bound for $m_{H_2^0}$ (the lower bound is zero) as a function of $m_{H_3^0}$. Upper and lower bounds are obtained by varying the free parameters with the constraint that all physical Higgs squared masses are positive. Note that, with the exception of $m_{H_2^0}$, the value of $m_{H_3^0}$ almost completely determines the other Higgs-boson masses for a given choice of $m_{Z'}$ and $\tan\beta$. Indeed, $H^\pm$ and one of the heavier neutral Higgs bosons are always nearly degenerate with H_3^0, while the other heavy scalar Higgs boson is always nearly degenerate with the Z'. The neutral scalar degenerate with H_3^0 and $H^\pm$ is denoted by $H^0_{\rm deg}$ and that degenerate with Z' by $H^0_{Z'}$. "Level crossing" obviously takes place in the vicinity of $m_{H_3^0}\approx m_{Z'}$. The tightly constrained nature of the mass spectrum arises through the mass matrix diagonalization, from which we find that $m^2_{H_2^0}$ is only positive for a very narrow range of $m_{H^\pm}$ (or, equivalently, λ) at a fixed value of $m_{H_3^0}$.

The neutral-Higgs-scalar-mass spectrum given in Fig. 1 has been computed numerically by diagonalizing the Higgs-boson mass matrix. One can also obtain approximate analytic formulas for the masses which are accurate at the $\sim 10\%$ level for all values of $m_{H_3^0}$, so long as $m_{Z'}\gtrsim 0.4$ TeV. For large $m_{H_3^0}$ these formulas are valid to $\sim 1\%$. For instance, at $m_{Z'}=1$ TeV, $m_{H_3^0}\gtrsim 300$ GeV is sufficient for 1% accuracy, while at $m_{Z'}=0.6$ TeV (0.2 TeV), $m_{H_3^0}\gtrsim 180$ GeV ($\gtrsim 100$ GeV) is adequate. The formulas are derived using perturbation theory to second order as follows. The zeroth-order mass matrix is defined by keeping only terms of order λAn or n^2. The remainder of the mass matrix is treated as a perturbation. This expansion is appropriate in the limit where $n \gg v_1, v_2$, with no restriction on the size of λA compared to n. First, for the light Higgs boson,

$$m^2_{H_2^0}\approx m^2_{Z_{\rm SM}}\cos^2 2\beta + \frac{2m_W^2}{g^2}\left[\lambda^2\sin^2 2\beta+\frac{g_1^2}{18}(1+3\sin^2\beta)^2\right]-\frac{25g_1^2}{18}\gamma^2 , \tag{6}$$

where

$$\gamma=\frac{18\sqrt{2}m_W}{25gg_1^2}\left[\frac{\lambda A}{n}\sin 2\beta-2\lambda^2+\frac{5g_1^2}{18}(1+3\sin^2\beta)\right] . \tag{7}$$

The other neutral-Higgs-boson masses are given by

$$\begin{aligned} m^2_{H^0_{Z'}} &\approx m^2_{Z'}+\frac{\lambda A m_W^2\sin 2\beta}{g^2 n} + \frac{25g_1^2}{18}\gamma^2+\left[\frac{25g_1^2}{18}-\frac{2\lambda A}{n\sin 2\beta}\right]\rho^2 , \\ m^2_{H^0_{\rm deg}} &\approx \frac{2\lambda An}{\sin 2\beta}+\left[m^2_{Z_{\rm SM}}+\frac{g_1^2-8\lambda^2}{4g^2}m_W^2\right]\sin^2 2\beta - \left[\frac{25g_1^2}{18}-\frac{2\lambda A}{n\sin 2\beta}\right]\rho^2 , \end{aligned} \tag{8}$$

where

$$\rho=\frac{\sqrt{2}m_W}{g\left[\frac{25}{18}g_1^2-\frac{2\lambda A}{n\sin 2\beta}\right]}\left[\frac{\lambda A}{n}\cos 2\beta+\frac{5}{12}g_1^2\sin 2\beta\right] . \tag{9}$$

(The corresponding eigenvectors for these mass eigenstates will be given later.) These approximate analytic forms, which are very close to the exact results at large $m_{Z'}$ and $m_{H_3^0}$, are useful in understanding some of the basic points made below. Important points which we wish to note are that

$$\frac{\gamma}{n},\frac{\rho}{n}\ll 1 , \tag{10}$$

for $m_{Z'}\gtrsim 0.4$ TeV, as long as $\lambda\lesssim 1$, and that γ changes sign as λ varies between the minimum and maximum values allowed at a given $m_{H_3^0}$. However, if λ is large, i.e., very large $m_{H_3^0}$ values are allowed, then γ/n can be a substantial fraction of 1 when λ takes on its minimum

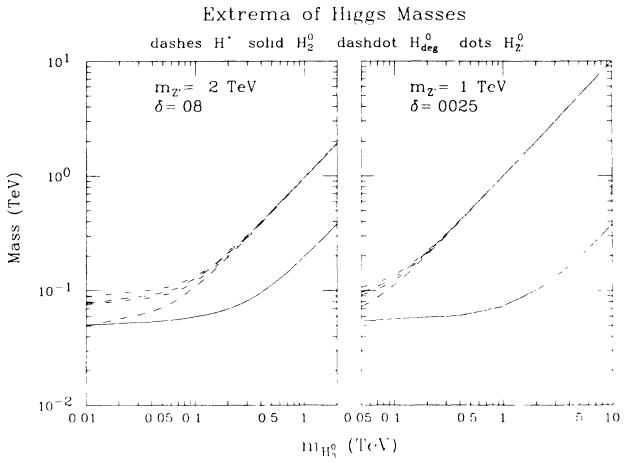

FIG. 1. Plots of upper and lower bounds for Higgs-boson masses, as a function of $m_{H_3^0}$ for $m_{Z'}=0.2$ TeV and $m_{Z'}=1.0$ TeV. The dashed curve is buried under the dashed-dotted curve for $m_{H_3^0}\gtrsim m_{Z'}$. The solid curve corresponds to the *upper* bound for $m_{H_2^0}$; the lower bound for $m_{H_2^0}$ is zero. The allowed mass regions are mapped out as λ (or, equivalently, $m_{H^\pm}$) is varied at any fixed $m_{H_3^0}$, and are determined by requiring that the lightest neutral scalar Higgs boson H_2^0 have positive mass squared.

and maximum values for the given $m_{H_3^0}$. Thus, in some of our later asymptotic results for couplings we shall retain terms of order γ/n, if there are no leading-order contributions.

As can be seen from Fig. 1, in the absence of restrictions on λ and λA, the maximum value of $m_{H_2^0}$ can be arbitrarily large; one need only take an appropriately large value for $m_{H_3^0}$. This follows also from Eqs. (5), (6), and (7). To see this one must combine these equations and look for those values of λ for which $m_{H_2^0}^2 > 0$. One finds, as illustrated in Fig. 2, that (at fixed $m_{Z'}$, i.e., at fixed n) λ must grow with $m_{H_3^0}$:

$$\lambda_{\max,\min} \simeq \frac{5}{4}\left\{\frac{1}{5}\left[\frac{m_3 s_{2\beta}}{n}\right]^2 + \frac{g_1^2}{9}(1+8s_\beta^2-5s_\beta^4) \pm \left[\frac{g_1^2}{18}\left[\frac{m_3 s_{2\beta}^2}{n}\right]^2 + \left[\frac{g_1^2}{9}\right]^2 (1+8s_\beta^2-5s_\beta^4)^2 - \frac{g^2 c_{2\beta}^2}{9\cos^2\theta_W}\right]^{1/2}\right\}, \tag{11}$$

where we have used the shorthand notation $m_3 = m_{H_3^0}$, $c_\beta = \cos\beta$, $s_\beta = \sin\beta$, $s_{2\beta} = \cos 2\beta$, and $c_{2\beta} = \cos 2\beta$. Note that to leading order in $m_{H_3^0}/n$ we have

$$\lambda \sim \frac{m_{H_3^0} \sin 2\beta}{2n} . \tag{12}$$

The minimum and maximum values of λ obtained in Eq. (11) lead to the small wedge of allowed λ values seen in the figure. For λ values in this wedge, the leading terms at large $m_{H_3^0}$ in γ cancel and the maximum $m_{H_2^0}$ value grows linearly with $m_{H_3^0}$. Since λ grows as $m_{H_3^0}$, it can be demonstrated from Eq. (5) that A (which is related to the scale of supersymmetry breaking) also grows proportionally to $m_{H_3^0}$, as seen in Fig. 2. The increase of λ and A with $m_{H_3^0}$ implies that we can obtain additional constraints on all Higgs-boson masses by applying various theoretically motivated restrictions on λ and A. First, we should demand that the $SU(2)_L \times U(1)_Y \times U(1)_{Y'}$ vacuum be a true minimum of the low-energy theory. (In particular, electric charge and color must be conserved.) Although there is some model dependence, one typically finds[4] after applying a full renormalization-group analysis that this requires that A be no larger than the gravitino mass, $A \lesssim O(m_{3/2})$. Second, λ (evaluated at the weak-boson-mass scale) may be bounded by insisting on perturbative unification. Various authors have obtained[2,6,8]

$$\lambda \lesssim 0.65-1.0 , \tag{13}$$

depending upon the precise definition of perturbative unification. By examining the maximum and minimum values of λ as a function of $m_{H_3^0}$, as well as the corresponding extrema of A, at each value of $m_{H_3^0}$, the impact of the constraints discussed above can be determined.

We first consider the effect of a bound on A. An examination of typical model solutions and the resulting $m_{3/2}$ values[3,4] suggests that a reasonable bound on A might be $|A| \lesssim 1$ TeV. From Fig. 2 this implies $m_{H_3^0} \lesssim 1.2$ or 1.4 TeV for $m_{Z'} = 0.2$ or 1.0 TeV, respectively. For asymptotically large $m_{Z'}$, we have determined numerically that the above bound on $|A|$ yields an upper bound on $m_{H_3^0}$ which is around 1 TeV. From Fig. 1 we see that such an upper bound on $m_{H_3^0}$ would imply upper bounds on the masses of $H^\pm$, H^0_{deg}, and H_2^0. These bounds become independent of $m_{Z'}$ for $m_{Z'} \gg 1$ TeV.

The constraints from Eq. (13) are also easily analyzed. To first approximation Fig. 2 shows that a given value of λ corresponds to a value for the maximum H_2^0 mass, which is independent of $m_{Z'}$, and to values of A, $m_{H^0_{\text{deg}}}$, $m_{H^\pm}$, and $m_{H_3^0}$ that scale with $m_{Z'}$. In particular, to restrict $m_{H_2^0}$ to lie below about 108 GeV it is sufficient to require $\lambda \lesssim 0.6$, independent of $m_{Z'}$. In fact, explicit models typically result in values of $\lambda \lesssim 0.1$ (Refs. 2 and 4), which restricts $m_{H_2^0}$ even further. In contrast, $m_{H_3^0} \gtrsim m_{Z'}$

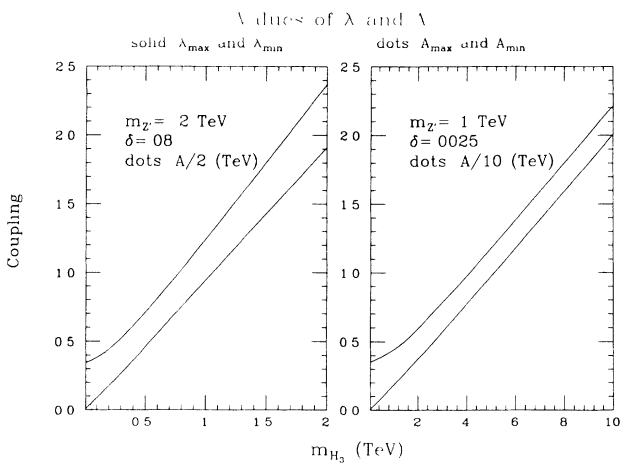

FIG. 2. Plots of λ and A. Solid curves give the maximum and minimum values of λ for a given $m_{H_3^0}$, and correspond to $m_{H_2^0} = 0$. The dotted curves give the maximum and minimum values of A (corresponding to $\lambda_{\min}$ and $\lambda_{\max}$, respectively). The allowed regions shown correspond to parameter values such that all Higgs bosons have positive mass squared.

is generally allowed by Eq. (13), and for $m_{Z'} \gtrsim 1$ TeV all Higgs bosons other than H_2^0 could lie above 1 TeV in the absence of any upper bound on $|A|$.

In general, a bound on λ is more restrictive than a bound on $|A|$ when the Z' is light, and vice versa when the Z' is heavy. In combination, such bounds imply relatively light Higgs-boson masses when $m_{Z'}$ is small. However, even when $m_{Z'}$ is large, they require that H_2^0 be light and that $m_{H_3^0}$, $m_{H^0_{\rm deg}}$, and $m_{H^\pm}$ all be below ~ 1 TeV. We note that further constraints on the Higgs-boson masses would be obtained from a renormalization-group analysis with specific boundary conditions. A few scenarios of this type were analyzed in Ref. 7, yielding results consistent with our general analysis.

In the absence of bounds on λ or A, it is still necessary to verify that the potential V has a lower value when the Higgs fields acquire VEV's than the $V=0$ value appropriate to the unbroken symmetry phase. Thus we have computed $\langle V \rangle$, the value of V when the Higgs bosons are assigned their respective VEV's, as a function of $m_{H_3^0}$ and λ (or $m_{H^\pm}$) for various values of $m_{Z'}$. At $m_{Z'}=0.2$ TeV, we find that $\langle V \rangle$ becomes positive for $m_{H_3^0}$ just below the 2-TeV limits of our plot in Fig. 1, while for $m_{Z'}=0.6$ TeV $\langle V \rangle$ remains negative up to $m_{H_3^0} \sim 18$ TeV and for $m_{Z'}=1$ TeV up to $m_{H_3^0} \sim 50$ TeV. More details concerning the behavior of $\langle V \rangle$ as a function of $m_{H_3^0}$ can be found in Ref. 20.

Of course, experimental results from the SLAC Linear Collider (SLC) and from the CERN collider LEP I will help enormously to reduce the parameter space that must be considered when exploring implications for a future high-energy collider, such as an e^+e^- linear collider with $\sqrt{s} \sim 1$ TeV or the Superconducting Super Collider (SSC). We see from the above analysis that there are two possible results in the context of the present model.

(1) Since the H_2^0 is predicted to be light, it may well be discovered at SLC and LEP I, which are expected to be sensitive to Higgs bosons with mass up to ~ 40 GeV. This assumes standard-model (SM) couplings, which we will demonstrate are characteristic of the H_2^0. In this case $m_{H_2^0}$ will be known and there will be only a twofold ambiguity in the values of λ (which implies a twofold ambiguity in A and all other parameters) at a given $m_{H_3^0}$. However, as seen from Fig. 1, a measurement of $m_{H_2^0}$ in the range $m_{H_2^0} \lesssim 50$ GeV will not place a lower bound on $m_{H_3^0}$. LEP II could potentially observe H_2^0 up to masses of order 80 GeV. Any $m_{H_2^0}$ mass above ~ 50 GeV will imply a lower limit on $m_{H_3^0}$.

(2) Alternatively, SLC, LEP I, and LEP II may place a lower bound on a SM-coupled Higgs boson, such as $m_{H_2^0} \gtrsim 80$ GeV. This, coupled with upper bounds on $m_{H_3^0}$, as discussed above, would imply a restricted range of $m_{H_3^0}$ consistent with experiment and theoretical constraints, and would imply that at each $m_{H_3^0}$ the parameter $m_{H^\pm}$ (or equivalently λ) could only take on a very narrow range of values.

To illustrate the possibilities, we shall frequently discuss results in the case that one has a bound of $m_{H_2^0} \geq 40$ GeV. Often, as will be mentioned when appropriate, very similar results obtain if the $m_{H_2^0}$ mass were known to be 40 GeV.

III. NEUTRALINOS AND CHARGINOS IN THE E_6 MODEL

In addition to the Higgs sector there are many other particles associated with the E_6-based supersymmetric theories. These include the gluino, squarks, sleptons, gauginos, and Higgsinos. The gauginos and Higgsinos are the spin-$\frac{1}{2}$ partners of the W; the γ, Z, and Z'; and the Higgs fields $H_1^{(a)}$, $H_2^{(a)}$, $N_1^{(a)}$, and $N_2^{(a)}$ ($a=1,2,3$ is the multiplet generation index as before). They mix to form the particles termed neutralinos and charginos. In this paper, we focus on those aspects of the above particles that determine their importance in Higgs-boson decays.

Generally speaking, Higgs-boson tree-level decays will include supersymmetric final states, such as squark pairs, slepton pairs, and neutralino/chargino pairs. However, we argue that for a first survey it is appropriate to retain only the neutralino/chargino final states. First, the squarks and sleptons are expected to be significantly more massive than the neutralinos and charginos that will dominate Higgs-boson decays. Second, the couplings of the squarks and sleptons are such that, even when phase space allowed, a Higgs boson prefers to decay to a neutralino/chargino pair. Roughly, the latter type channel is enhanced (relative to squark final states) by a factor of m_H^2/m_V^2, where m_H is the Higgs-boson mass and m_V is the mass of one of the gauge bosons of the theory. Thus, we shall consider in detail the neutralino/chargino sector of the theory.

The mass spectrum of the neutralinos and charginos is critical in determining their importance as final states in Higgs-boson decays. The mass matrices of this sector are greatly simplified by the basis choice that we made earlier for the Higgs fields. In that basis, the mass matrix for both charginos and neutralinos breaks up into two components: one involving the gauginos and the third-generation Higgsinos; and a second that determines the masses and mixings of the first- and second-generation Higgsinos. As we shall shortly see, the gaugino–third-generation-Higgsino mass matrix is very closely tied to the Higgs-boson sector and the parameters that occur there. Masses for the Higgsinos associated with first and second generations are more model dependent, being determined by the intergenerational trilinear superpotential couplings λ_{ij3}, λ_{i3j}, and λ_{3ij}, $i,j=1,2$. An important question is whether these first- and second-generation Higgsinos can be important in Higgs-boson decays. In the basis we employ, such decays arise through these same λ_{ij3}-type couplings, and through possible intergenerational mixing in the gaugino–Higgsino–Higgs-boson couplings. The sizes of these two types of generation mixing terms are uncertain. Our approach, in this first survey of Higgs-boson decays, will be to assume that they

are significantly smaller than the intragenerational decays we consider. However, as outlined below, this is only a first approximation. Though we shall not attempt any detailed discussion in this paper, in this same approximation it is the gaugino–third-generation-Higgsino sector that is most important in the decays of heavy squarks and gluinos, since the latter particles are most strongly coupled to the gaugino components of the neutralinos and charginos.

The most significant constraints upon intergenerational mixing are those upon the λ_{ij3}-type couplings. First, the lightest chargino in the first- and second-generation sector cannot have mass less than the experimental lower bound which is roughly 30 GeV. [We use the above bound as a conservative limit based on the DESY PETRA bound of 23 GeV (Ref. 21) and the limit of Ref. 22, inferred from UA1 data, of $\sim$40 GeV.] Reference 7 discusses this constraint with the conclusion that λ_{ii3} can be quite small. Bounds from the neutralino sector of the first and second generations are less concrete. It has been argued[23] that the lightest neutralino (including all three families) must have large gaugino components if its relic cosmological density is not to exceed the critical density. We believe that it is also possible to have a lightest supersymmetric particle (LSP) which is dominantly third-generation Higgsino if it is more massive than the top quark. One may then be able to ensure that relic Higgsinos are not overabundant due to annihilation into $t\bar{t}$ pairs in the early Universe.[24] [Note that such a mechanism is not available for Higgsinos of the first two generations due to their presumed small couplings to fermions and their superpartners, which are needed to ensure suppressed flavor-changing neutral currents (FCNC's).] In either case, this means that the LSP should belong to our gaugino–third-generation-Higgsino sector. If one requires that the lightest Higgsino from the first and second generations be more massive than the lightest third-generation neutralino, a lower bound on the λ_{ij3}-type coupling ($i \neq j$) is obtained, that, depending upon the mass of the lightest gaugino, can be significant. For the remainder of this paper, we shall assume that intergenerational mixing is relatively small.

Our assumption of small intergenerational couplings will have important implications for Higgs-boson detection via its decays into neutralinos and charginos. These final-state particles will subsequently decay into either two-body final states via $\tilde{\chi}_i \to \tilde{\chi}_j +$gauge or Higgs bosons if kinematically allowed, or via three-body decays: $\tilde{\chi}_i \to \tilde{\chi}_j f\bar{f}$ (due to virtual exchange of $\tilde{f}$ and gauge bosons). In each case above, $\tilde{\chi}_i$ and $\tilde{\chi}_j$ are eigenstates produced by gaugino and third-family Higgsino mixing; whereas, f is a quark or lepton of arbitrary generation. These decays will continue until the lightest such $\tilde{\chi}$ is produced. Since we have argued that this lightest (neutral) $\tilde{\chi}$ is in fact the lightest supersymmetric particle, no further decays will occur, and to first approximation Higgs-boson decays would not yield neutralinos and charginos associated with the Higgsinos of the first and second generation. (Should the lightest neutral $\tilde{\chi}$ of the third-generation-Higgsino–gaugino mixing sector not be the true LSP, it would tend to decay via off-diagonal λ's to $\tilde{\chi}$'s, that are dominantly first- or second-generation Higgsinos, plus an unhiggs boson from the first or second generation.) Thus, we now turn our attention to a detailed discussion of the charginos and neutralinos emerging from the gaugino–third-generation-Higgsino sector, as being crucial to an understanding of Higgs-boson decay phenomenology.

In general, all the gauginos and the (third-family) Higgsinos of a given charge mix with one another, and the mass eigenstates must be determined by diagonalizing the mass matrix. Under the assumption that N_2 does not acquire a vacuum expectation value the fermionic partner of N_2 remains unmixed leaving us with two mass matrices: a 2×2 matrix for the chargino partners of the $W^{\pm}$ and charged Higgs boson; and a 6×6 matrix for the neutralinos. It is here that a great simplification occurs in the E_6-based models in comparison to an arbitrary supersymmetric theory with the same fields. Namely, we need specify only the sign of λ and one additional parameter beyond those already discussed in order to completely specify all these mass matrices. The above statement is true provided there is no intermediate scale of symmetry breaking between the grand unification scale and the electroweak scale. In this case the various gaugino masses, which are equal at the grand unification scale, can be related at the electroweak scale by

$$\frac{3}{5}\frac{M_1}{g_1^2} = \frac{3}{5}\frac{M'}{g'^2} = \frac{M}{g^2} = \frac{M_{\tilde{g}}}{g_s^2} , \tag{14}$$

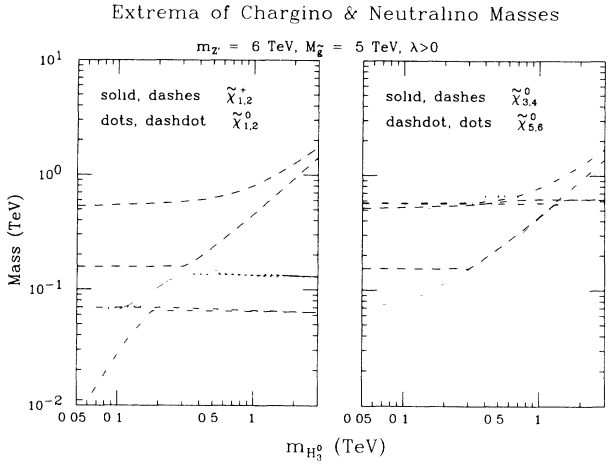

FIG. 3. We plot, as a function of $m_{H_3^0}$, the upper and lower bounds of the masses of all the neutralino and chargino eigenstates associated with the gauginos and Higgsinos. In all there are 8 states. The first plot shows the masses for the two charginos and the two lightest neutralinos. The second shows the masses for the remaining four neutralinos. We have chosen $m_{Z'}=0.6$ TeV and $M_{\tilde{g}}=0.5$ TeV. The upper and lower bounds are obtained analogously to those in Fig. 1 by varying $m_{H^{\pm}}$ (or equivalently λ), at fixed $m_{H_3^0}$, through the range for which $m^2_{H_2^0} > 0$. The sign of λ has been taken to be positive. Note that many of the curves are overlapping due to the near degeneracy of many of the eigenstates.

where M_1, M', M, and $M_{\tilde{g}}$ are the soft-supersymmetry-breaking terms associated with the $U(1)_{Y'}$, $U(1)_Y$, $SU(2)_L$, and SU(3) subgroups. Thus, when discussing results for the neutralinos and charginos, we need only specify the sign of λ, and values for $M_{\tilde{g}}$ and g_s^2. [We shall take $\alpha_s \equiv g_s^2/(4\pi)=0.136$ and $\lambda>0$ for the forthcoming numerical analysis.]

Let us first give the chargino and neutralino mass matrices. (All Higgsino fields considered below belong to the third generation.) In the first case we employ the $\tilde{W}^{\pm}$-$\tilde{H}^{\pm}$ basis, and, in the second case, the $\tilde{W}_3$-$\tilde{B}'$-$\tilde{B}_1$-$\tilde{H}_1$-$\tilde{H}_2$-$\tilde{N}_1$ basis. The chargino mass matrix is then

$$X_C=\begin{bmatrix} M & gv_2 \\ gv_1 & -\lambda n \end{bmatrix}, \tag{15}$$

while that for the neutralinos is

$$X_N=\begin{bmatrix} M & 0 & 0 & \frac{gv_1}{\sqrt{2}} & -\frac{gv_2}{\sqrt{2}} & 0 \\ 0 & M' & 0 & -\frac{g'v_1}{\sqrt{2}} & \frac{g'v_2}{\sqrt{2}} & 0 \\ 0 & 0 & M_1 & \frac{g_1v_1}{3\sqrt{2}} & \frac{4g_1v_2}{3\sqrt{2}} & -\frac{5g_1n}{3\sqrt{2}} \\ \frac{gv_1}{\sqrt{2}} & -\frac{g'v_1}{\sqrt{2}} & \frac{g_1v_1}{3\sqrt{2}} & 0 & \lambda n & \lambda v_2 \\ -\frac{gv_2}{\sqrt{2}} & \frac{g'v_2}{\sqrt{2}} & \frac{4g_1v_2}{3\sqrt{2}} & \lambda n & 0 & \lambda v_1 \\ 0 & 0 & -\frac{5g_1n}{3\sqrt{2}} & \lambda v_2 & \lambda v_1 & 0 \end{bmatrix}. \tag{16}$$

These matrices are diagonalized by the operations $U^*X_CV^{-1}$ and $N^*X_NN^{-1}$ for the chargino and neutralino mass matrices, respectively. There are many possible conventions for U, V, and N. We choose to diagonalize in such a way that all masses turn out to be positive. In this case the diagonalizing matrices will, in general, be complex. The diagonalizing matrices described above will enter into various couplings to be given later.

Since renormalization-group investigations tend to suggest a large gluino mass[3,4] we will discuss here the results for $M_{\tilde{g}}=0.5$ TeV. Also, we will adopt the value of $m_{Z'}=0.6$ TeV (a value intermediate between those for which Higgs-boson masses were plotted in Fig. 1). In addition, we take λ to be positive; the negative sign for λ leads to slightly smaller masses. (For mass spectra in the $\lambda<0$ case see Refs. 20 and 25.) The results for the masses of all the neutralinos and charginos appear in Fig. 3, plotted as a function of $m_{H_3^0}$. We shall label states as $\tilde{\chi}_i^+$ ($i=1,2$) and $\tilde{\chi}_i^0$ ($i=1,6$) where i increases with mass. (An alternative labeling according to eigenvector content is given below.) As in the presentation of Higgs-boson masses in Fig. 1, we have given the upper and lower bounds for the mass of a given state at fixed $m_{H_3^0}$ obtained by varying $m_{H^{\pm}}$, or equivalently λ, through its allowed range. The resulting masses cover a broad spectrum.

(1) Once $m_{H_3^0} \gtrsim 0.3$ TeV, the two lightest neutralinos and the lightest chargino are predominantly gaugino, with masses that are primarily determined by M and M', and hence by $M_{\tilde{g}}$. Even for small $m_{H_3^0}$ values there are still two neutralino states that are dominantly $\tilde{W}_3$ and $\tilde{B}'$ gauginos and have masses of order M and M'; however, they are no longer necessarily the lightest neutralino states. Similarly, there is always a chargino which has mass $\sim M$; but this state is no longer necessarily the lightest once $m_{H_3^0}$ is small. It will be useful to establish a notation for these states which refers to their content. Thus we denote those neutralino states that have masses M, M' as $\tilde{\chi}^0_{\tilde{W}_3}, \tilde{\chi}^0_{\tilde{B}'}$, respectively, and the chargino state of mass M by $\tilde{\chi}^+_{\tilde{W}^+}$.

(2) Two of the neutralinos have masses determined by the Z' mass scale. These states are approximately degenerate, and have Higgsino content $\tilde{N}_1 \pm \tilde{B}_1$. In correspondence with their composition, they will be denoted by $\tilde{\chi}^0_{\tilde{N}_1+\tilde{B}_1}$ and $\tilde{\chi}^0_{\tilde{N}_1-\tilde{B}_1}$. These two states always have masses given approximately by $m_{Z'}-M_1/2$ and $m_{Z'}+M_1/2$, respectively.

(3) The other chargino and the final two neutralinos are predominantly composed of the Higgsino partners of the Higgs-doublet fields. At large $m_{H_3^0}$ they have masses that, to first rough approximation, are given by λn [which, at $\tan\beta \sim 1$, is roughly of order $m_{H_3^0}/2$, see Eq. (12)]. The two neutralino states are approximately equal mixtures of $\tilde{H}_1$ and $\tilde{H}_2$, while the chargino state is close to being pure $\tilde{H}^+$. We denote these states by $\tilde{\chi}^0_{\tilde{H}_1+\tilde{H}_2}$, $\tilde{\chi}^0_{\tilde{H}_1-\tilde{H}_2}$, and $\tilde{\chi}^+_{\tilde{H}^+}$. At large $m_{H_3^0}$, $\tilde{\chi}^0_{\tilde{H}_1+\tilde{H}_2}$ is slightly

heavier than $\tilde{\chi}^0_{\tilde{H}_1-\tilde{H}_2}$. To first approximation, varying $m_{Z'}$ leads to little change in their masses at a fixed value of $m_{H^0_3}$. Their masses are also essentially independent of $M_{\tilde{g}}$. As $m_{H^0_3}$ decreases, the eigenstate composition of these states changes relatively little, even if they undergo level crossing with the other neutralino or chargino states.

(4) Exactly how light $\tilde{\chi}^0_{\tilde{H}_1+\tilde{H}_2}$, $\tilde{\chi}^0_{\tilde{H}_1-\tilde{H}_2}$ and $\tilde{\chi}^+_{\tilde{H}^+}$ become at small $m_{H^0_3}$ is determined by the value of $m_{H^\pm}$ or, equivalently, λ, that is appropriate within the range allowed at the fixed $m_{H^0_3}$ being considered. If λ is near its minimum (which can be 0 or very small at small $m_{H^0_3}$), then $\tilde{\chi}^0_{\tilde{H}_1+\tilde{H}_2}$ will be the LSP ($\tilde{\chi}^0_1$) and $\tilde{\chi}^0_{\tilde{H}_1-\tilde{H}_2}$ and $\tilde{\chi}^+_{\tilde{H}^+}$ will be roughly degenerate at a slightly higher mass. As higher values for λ are chosen at a fixed small $m_{H^0_3}$ the masses of these states rise very rapidly when n is fairly large, and the gaugino state $\tilde{\chi}^0_{\tilde{B}'}$ becomes the LSP. Thus the cosmological argument for a gaugino LSP suggests that, perhaps, very small λ values are not allowed. However, this does not prevent a very small mass for the H^0_2, since $m_{H^0_2}$ is zero at the maximum allowed λ at a given $m_{H^0_3}$, as well as at the minimum allowed λ.

As discussed in the previous section, it is also possible to imagine that we will either shortly observe the H^0_2, or place a lower bound on its mass, in which case the chargino and neutralino masses are more constrained. To illustrate the possibilities, we take $m_{H^0_2} \geq 40$ GeV and plot chargino and neutralino masses as a function of $m_{H^0_3}$ in Fig. 4. We shall use this same H^0_2 mass choice and the associated neutralino/chargino mass spectrum in later sections. The results for this specific choice of $m_{H^0_2}$ differ in several important respects, in comparison to those of Fig. 3. First, the lightest neutralino can no longer have an arbitrarily small mass. This is true since, by placing a lower bound on $m_{H^0_2}$, we fix the minimum possible value of λ corresponding to a given $m_{H^0_3}$. As a result, the LSP is always the gaugino $\tilde{\chi}^0_{\tilde{B}'}$, independent of $m_{H^0_3}$. (As discussed earlier, cosmological arguments suggest that this might be a problem for large $M_{\tilde{g}}$ and, hence, large M', since a first- or second-generation neutralino might then be the true LSP.) Otherwise, the pattern remains much as in the unrestricted $m_{H^0_2}$ case, with $\tilde{\chi}^0_{\tilde{W}_3}$ and $\tilde{\chi}^+_{\tilde{W}^+}$ having mass $\sim M$, $\tilde{\chi}^0_{\tilde{N}_1+\tilde{B}_1}$, and $\tilde{\chi}^0_{\tilde{N}_1-\tilde{B}_1}$ having mass $\sim m_{Z'}$, and $\tilde{\chi}^0_{\tilde{H}_1+\tilde{H}_2}$, $\tilde{\chi}^0_{\tilde{H}_1-\tilde{H}_2}$ being approximately degenerate at a mass that asymptotes to $\sim m_{H^0_3}/2$ (for $\tan\beta \sim 1$).

Altogether, we have a neutralino/chargino mass spectrum that is closely tied to the Z' mass and the Higgs-boson mass spectrum. Since these neutralinos and charginos of the third generation are crucially important channels for Higgs-boson decays, this close interconnection will lead to interesting patterns in the Higgs-boson branching ratios.

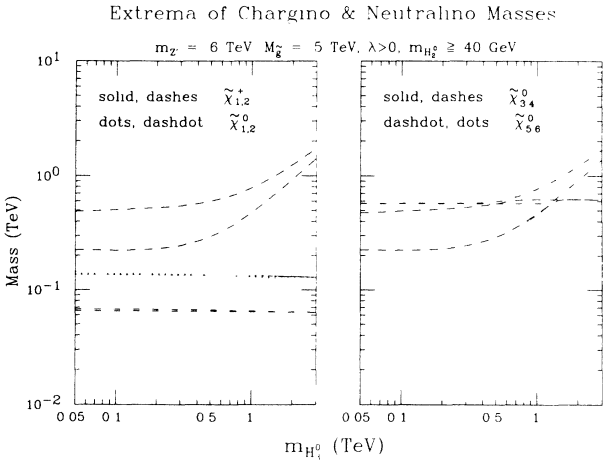

FIG. 4. We plot, as a function of $m_{H^0_3}$, the masses of all the neutralino and chargino eigenstates subject to the requirement that $m_{H^0_2}$ be ≥ 40 GeV. In all there are 8 states. The first plot shows the masses for the two charginos and two of the neutralinos. The second shows the masses for the remaining four neutralinos, including the two lighter ones. We have chosen $m_{Z'}=0.6$ TeV and $M_{\tilde{g}}=0.5$ TeV. The sign of λ has been taken to be positive. Note that many of the curves are overlapping due to the near degeneracy of many of the eigenstates.

IV. COUPLINGS OF HIGGS BOSONS TO $q\bar{q}$ AND VV' CHANNELS

A. Couplings of Higgs bosons to quark-antiquark channels

It is very straightforward to summarize the couplings of the Higgs bosons of this model to the various channels involving standard-model fermions. In addition, we include here the couplings of the various Higgs bosons to the extra exotic charge $-\frac{1}{3}$ quark that occurs in the 27 representation in which each SM generation resides. As stated earlier we assume that only the Higgs fields of the third generation acquire vacuum expectation values, and that it is these VEV's that lead to the quark and lepton masses. The results are given in third-family notation. The couplings of the (third-generation) Higgs bosons to quarks and leptons of other generations are obtained, in the usual way by using the appropriate values for the quark masses. (For simplicity, we will neglect the off-diagonal elements of the Kobayashi-Maskawa mixing matrix which are present in the charged-Higgs-boson–quark couplings.)

The Higgs-boson couplings depend on the Higgs eigenvectors obtained via the diagonalization process outlined in Sec. II. We define these eigenvectors to be $H_\alpha(i)$, where $\alpha=2,\text{deg},Z',3$ runs over the four possible labels corresponding to the neutral-Higgs-boson mass eigenstates and $i=1,2,3$, where the index i refers to the Lagrangian-basis states H_1, H_2, and N_1, respectively. In terms of these $\mathbf{H}_\alpha$'s the couplings of interest may be given. For the neutral Higgs boson the $H_\alpha q\bar{q}$ ($\alpha=2,\text{deg},Z',3$) couplings read

$$g_{t\bar{t}H^0_\alpha} = -\frac{gm_t}{2m_W \sin\beta} H_\alpha(2) ,$$
$$g_{b\bar{b}H^0_\alpha} = -\frac{gm_b}{2m_W \cos\beta} H_\alpha(1) . \quad (17)$$

(In the above, the H^0_3 couplings must be multiplied by a factor of $-i\gamma_5$.) For the $H^+t\bar{b}$ Feynman coupling we have

$$g_{H^+t\bar{b}} = \frac{g}{\sqrt{2}m_W}(m_t \cot\beta P_R + m_b \tan\beta P_L) , \quad (18)$$

where $P_{R,L} = (1 \pm \gamma_5)/2$. Finally, the singlet quark h couples to the physical Higgs bosons only through the singlet N_1:

$$g_{h\bar{h}H^0_\alpha} = -\frac{m_h}{\sqrt{2n}} H_\alpha(3) , \quad (19)$$

where $\alpha = 2, \text{deg}, Z', 3$.

Asymptotic results, valid for large $m_{Z'}$ and large $m_{H^0_3}$, for the above couplings, and other couplings to be considered later, may be obtained using approximate analytic forms for the $\mathbf{H}_\alpha$'s:

$$\mathbf{H}_2 \simeq \frac{1}{\left[1+\frac{\gamma^2}{n^2}\right]^{1/2}} \begin{pmatrix} \cos\beta \\ \sin\beta \\ \frac{\gamma}{n} \end{pmatrix} ,$$
$$\mathbf{H}_{Z'} \simeq \frac{1}{\left[1+\frac{\gamma^2+\rho^2}{n^2}\right]^{1/2}} \begin{pmatrix} -\frac{\gamma}{n}\cos\beta + \frac{\rho}{n}\sin\beta \\ -\frac{\gamma}{n}\sin\beta - \frac{\rho}{n}\cos\beta \\ 1 \end{pmatrix} ,$$
$$\mathbf{H}_{\text{deg}} \simeq \frac{1}{\left[1+\frac{\rho^2}{n^2}\right]^{1/2}} \begin{pmatrix} -\sin\beta \\ \cos\beta \\ \frac{\rho}{n} \end{pmatrix} , \quad (20)$$
$$\mathbf{H}_3 = \frac{1}{\left[1+\frac{1}{2}\sin^2 2\beta \frac{m_W^2}{g^2 n^2}\right]^{1/2}} \begin{pmatrix} \sin\beta \\ \cos\beta \\ \frac{1}{\sqrt{2}}\sin 2\beta \frac{m_W}{gn} \end{pmatrix} ,$$

where γ and ρ are defined in Eqs. (7) and (9). (Note that the $\mathbf{H}_3$ eigenvector is actually exact.) The $\mathbf{H}_2$, $\mathbf{H}_{\text{deg}}$, and $\mathbf{H}_{Z'}$ eigenvectors are computed to first order using the perturbation expansion of the mass matrix briefly described in Sec. II, and are valid to 4% for $m_{H^0_3} \gtrsim 0.3$ TeV at $m_{Z'} = 1$ TeV and for $m_{H^0_3} \gtrsim 0.2$ TeV for $m_{Z'} = 0.6$ TeV. As $m_{H^0_3}$ increases beyond the indicated values, the eigenvectors at first become increasingly accurate, but eventually, when $m_{H^0_3}$ becomes extremely large (well beyond the values plotted in any of the graphs we shall show) γ/n can become $\gtrsim 1$ when λ takes on values near either its allowed minimum or maximum, and the approximate forms for $\mathbf{H}_2$ and $\mathbf{H}_{Z'}$ given above will no longer be accurate. Over the range of $m_{H^0_3}$ of interest here, however, the above forms may be used. Substituting these forms into the quark coupling equations, and taking $\tan\beta \sim 1$ as an example, yields the following results.

(1) First, the $H^+b\bar{t}$ Feynman coupling is simply obtained from Eq. (18) with $\tan\beta = 1$.

(2) For the $H^0_{\text{deg}}q\bar{q}$, $H^0_2 q\bar{q}$, and $H^0_3 q\bar{q}$ couplings we have SM-like strength of order $gm_q/(2m_W)$.

(3) For the $H^0_{Z'}h\bar{h}$ coupling we have a value controlled by $m_{Z'}$:

$$g_{h\bar{h}H^0_{Z'}} \sim \tfrac{5}{6} g_1 m_h / m_{Z'} . \quad (21)$$

We restrict q above to be either b or t, while h denotes the exotic quark described previously. Couplings not listed are approximately zero. In particular, H^0_2, H^0_{deg}, and H^0_3 have ~ 0 coupling to $h\bar{h}$, while $H^0_{Z'}$ has ~ 0 coupling to any $q\bar{q}$. In principle, there are three generations of h quarks, each with the indicated coupling strength to $H^0_{Z'}$. We will assume that the mass of the third-generation h quark, which we take to be $m_h = 250$ GeV, is significantly larger than those of the first and second generation. If this is not true our branching ratios for the $h\bar{h}$ decay mode of the $H^0_{Z'}$, presented later, would have to be increased.

B. Couplings of Higgs bosons to vector-boson pairs

One of the important roles of the Higgs boson of the SM is to cure the bad high-energy behavior of the scattering amplitudes for longitudinally polarized W's and Z's. As a consequence, the Higgs coupling to WW and ZZ is very substantial and the SM Higgs-boson decays will be dominated by vector-boson pair channels whenever they are phase-space allowed. In the E_6 model we are discussing here, there are three neutral scalar Higgs bosons and it is important to know which (or what combination) of them is responsible for preserving unitarity in the WW, ZZ, ZZ', and $Z'Z'$ scattering amplitudes. Similar considerations apply to the $Z'W^\pm$ scattering channels, whose bad high-energy behavior is cured by the $H^\pm$. *A priori*, one only knows that

$$\sum_i g^2_{H_i VV'} = C_{VV'} , \quad (22)$$

where $C_{VV'}$ has a definite value for every VV' scattering channel. We give below the results for these sum rules in the limit of large $m_{Z'}$, i.e., large n:

$$C_{W^+W^-} = g^2 m_W^2 ,$$
$$C_{ZZ} = \frac{g^2 m^2_{Z_{\text{SM}}}}{\cos^2\theta_W} ,$$
$$C_{ZZ'} = \frac{g_1^2 m^2_{Z_{\text{SM}}}}{9}(\cos^2\beta + 16\sin^2\beta) , \quad (23)$$
$$C_{Z'W^\pm} = \tfrac{25}{36} g_1^2 m_W^2 \sin^2 2\beta ,$$
$$C_{Z'Z'} = \tfrac{25}{9} g_1^2 m^2_{Z'} .$$

The W^+W^- sum rule is exact, independent of the value

of $m_{Z'}$; in the other channels it is only the mixing of the neutral gauge bosons that would make the exact formulas complicated.

The explicit couplings of the various Higgs bosons may be given in terms of the eigenvectors of the Higgs-boson mass eigenstates, H_α, for which approximate forms were given in Eq. (20). The couplings are given below. The $g_{H_\alpha W^+W^-}$, $\alpha=2,\text{deg},Z'$ couplings are

$$g_{H_\alpha W^+W^-}=gm_W[\cos\beta H_\alpha(1)+\sin\beta H_\alpha(2)] . \quad (24)$$

The neutral vector-boson couplings are more complicated, due to the extra U(1) factor in the low-energy group.

For the ZZ channel,

$$g_{H_\alpha ZZ}=\frac{v_1}{\sqrt{2}}\left[\frac{g\cos\delta}{\cos\theta_W}+\frac{g_1}{3}\sin\delta\right]^2 H_\alpha(1) + \frac{v_2}{\sqrt{2}}\frac{g\cos\delta}{\cos\theta_W}\left[\frac{g\cos\delta}{\cos\theta_W}-\frac{8}{3}g_1\sin\delta\right]H_\alpha(2) + \frac{25n}{9\sqrt{2}}g_1^2\sin^2\delta H_\alpha(3) . \quad (25)$$

For the ZZ' channel,

$$g_{H_\alpha ZZ'}=\frac{v_1}{\sqrt{2}}\left[\frac{gg_1}{\cos\theta_W}\cos2\delta+\frac{\sin2\delta}{2}\left[\frac{g_1^2}{9}-\frac{g^2}{\cos^2\theta_W}\right]\right]H_\alpha(1)-\frac{gv_2}{\sqrt{2}\cos\theta_W}\left[\frac{4}{3}g_1\cos2\delta+\frac{g\sin2\delta}{2\cos\theta_W}\right]H_\alpha(2) + \frac{25n}{18\sqrt{2}}g_1^2\sin2\delta H_\alpha(3) . \quad (26)$$

For the $Z'Z'$ channel,

$$g_{H_\alpha Z'Z'}=\frac{v_1}{\sqrt{2}}\left[\frac{g\sin\delta}{\cos\theta_W}-\frac{g_1}{3}\cos\delta\right]^2 H_\alpha(1) + \frac{v_2}{\sqrt{2}}\frac{g\sin\delta}{\cos\theta_W}\left[\frac{g\sin\delta}{\cos\theta_W}+\frac{8}{3}g_1\cos\delta\right]H_\alpha(2) + \frac{25n}{9\sqrt{2}}g_1^2\cos^2\delta H_\alpha(3) . \quad (27)$$

Finally, for the $W^\pm Z$ and $W^\pm Z'$ channels we have

$$g_{H^\pm W^\mp Z}=\tfrac{5}{6}g_1 m_W\sin2\beta\sin\delta ,$$
$$g_{H^\pm W^\mp Z'}=\tfrac{5}{6}g_1 m_W\sin2\beta\cos\delta . \quad (28)$$

The HVV' couplings will be key ingredients in determining the decay patterns of these Higgs bosons. For large n and small neutral-gauge-boson mixing δ the approximate eigenvectors of Eq. (20) may be used to obtain very simple and easily summarized results for all the above couplings. For the W^+W^- channel we have

$$g_{H_2^0W^+W^-}\simeq gm_W ,$$
$$g_{H^0_{\text{deg}}W^+W^-}\simeq 0 , \quad (29)$$
$$g_{H_{Z'}^0W^+W^-}\simeq -\frac{\gamma}{n}gm_W .$$

For the ZZ channel the couplings are

$$g_{H_2^0ZZ}\simeq\frac{gm_{Z_{\text{SM}}}}{\cos\theta_W} ,$$
$$g_{H^0_{\text{deg}}ZZ}\simeq 0 , \quad (30)$$
$$g_{H_{Z'}^0ZZ}\simeq -\frac{\gamma}{n}\frac{gm_{Z_{\text{SM}}}}{\cos\theta_W} .$$

For the ZZ' channel we have

$$g_{H_2^0ZZ'}\simeq\frac{g_1 m_{Z_{\text{SM}}}}{3}(\cos^2\beta-4\sin^2\beta) ,$$
$$g_{H^0_{\text{deg}}ZZ'}\simeq -\tfrac{5}{6}g_1 m_{Z_{\text{SM}}}\sin2\beta , \quad (31)$$
$$g_{H_{Z'}^0ZZ'}\simeq\frac{g_1 m_{Z_{\text{SM}}}}{3}\left[\frac{\gamma}{n}(4\sin^2\beta-\cos^2\beta)+\frac{5\rho}{2n}\sin2\beta\right] .$$

For the $Z'Z'$ channel we obtain

$$g_{H_2^0Z'Z'}\simeq\frac{2\sqrt{2}g_1}{\cos\theta_W}(\sqrt{2}m_W\cos^2\beta+25g\gamma) ,$$
$$g_{H^0_{\text{deg}}Z'Z'}\simeq\frac{g_1^2}{9\sqrt{2}}\left[-\frac{m_W\sin2\beta}{\sqrt{2}g}+25\rho\right] , \quad (32)$$
$$g_{H_{Z'}^0Z'Z'}\simeq\tfrac{5}{3}g_1 m_{Z'} .$$

Finally, for the $W^\mp Z$ and $W^\mp Z'$ channels we obtain

$$g_{H^\pm W^\mp Z}\simeq 0 ,$$
$$g_{H^\pm W^\mp Z'}\simeq\tfrac{5}{6}g_1 m_W\sin2\beta . \quad (33)$$

The couplings of the charged Higgs boson to $Z'W^\pm$ and of the neutral Higgs boson to $Z'Z$ are of particular phenomenological importance, in that they lead to decays

of the type $Z' \to HV$. It will be helpful to define certain normalized couplings. We begin with H_2^0 and write

$$f_{H_2^0 Z} \equiv \frac{|g_{Z'H_2^0 Z}|}{g m_{Z_{\rm SM}}} . \tag{34}$$

The dependence of $f_{H_2^0 Z}$ on $m_{Z'}$ and $m_{H_3^0}$ was considered in Ref. 5. For example, for the case of a very light Z', $m_{Z'}=0.2$ TeV, $f_{H_2^0 Z}$ ranged from ~ 0.2 to ~ 0.4 as $m_{H_3^0}$ was varied up to 1 TeV. For higher $m_{Z'}$, the range of values found for $f_{H_2^0 Z}$ quickly narrows, and the asymptotic result of Eq. (31) can be employed, yielding (at $\tan\beta \sim 1$) $f_{H_2^0 Z} \sim 0.5 \tan\theta_W \sim 0.27$, except for very small $m_{H_3^0}$ values. (To see what happens for small $m_{H_3^0}$, the reader is referred to Fig. 4 of Ref. 5.) Similarly, we define

$$f_{H^\pm W^\mp} \equiv \frac{|g_{Z'H^\pm W^\mp}|}{g m_W} \tag{35}$$

and

$$f_{H^0_{\rm deg} Z} \equiv \frac{|g_{Z'H^0_{\rm deg} Z}|}{g m_{Z_{\rm SM}}} . \tag{36}$$

These have been considered as a function of $m_{Z'}$, at selected values of $m_{H_3^0}$, in Ref. 5. The first is always close to the large $m_{H_3^0}$ asymptotic result obtained from the results given earlier, $\sim \frac{5}{6}\tan\theta_W \sim 0.45$, while the second lies in the range ~ 0.45 to ~ 0.6 at low $m_{Z'}$ and approaches the same asymptotic limit (at $\tan\beta \sim 1$). We shall see that the squares of the f_{HV}'s control the decay of the Z' to a HV channel. Hence, if phase space effects are ignored, one finds at large $m_{Z'}$ (and $\tan\beta \sim 1$) a ratio of 9:25:50 for $H_2^0 : H^0_{\rm deg} : H^\pm$ in Z' decays.

Of course, the mass spectrum of the Higgs bosons is such that it is also possible to have (at high $m_{H_3^0}$) $m_{H^0_{\rm deg}} > m_{Z'} + m_Z$ and $m_{H^\pm} > m_{Z'} + m_W$. In this case the significant size of the $ZZ'H^0_{\rm deg}$ and $W^\pm Z' H^\mp$ couplings will imply that the ZZ' and W^+Z' channels will be important in $H^0_{\rm deg}$ and H^+ decays, respectively. (Note, that, to the extent that Z-Z' mixing is small, the H^+ does not couple to ZW^+. The absence of this latter coupling is a common feature of models with only doublets, e.g., the minimal supersymmetric model described in Ref. 11.)

Another important class of couplings for both production and decay are those of the neutral Higgs bosons to W^+W^- and ZZ, for which we have given asymptotic results above. Asymptotically, we see that the WW and ZZ channels couple primarily to H_2^0 (which, given any reasonable bounds on λ and/or λA, will be too light to decay in these modes), but can have small couplings to $H_{Z'}^0$. However, these asymptotic results are not accurate for small $m_{H_3^0}$ and/or small $m_{Z'}$. Thus, we plot in Fig. 5 the extrema of these couplings relative to the SM coupling strength of $g m_W$, as we vary the parameters within their allowed domains. (The ZZ couplings have essentially the same ratio to the SM strength of $g m_{Z_{\rm SM}}/\cos\theta_W$.) That the WW and ZZ couplings to H_2^0 are of nearly SM strength is a feature well known in the minimal supersymmetric model.[12] It is not surprising that this continues to be true in the E_6 model (a fact which was also noted in Ref. 7). Note that outside the asymptotic domain there is considerable variation with $m_{Z'}$ and $m_{H_3^0}$; for instance, at small $m_{H_3^0}$ the $H^0_{\rm deg}$ (which is relatively light for such $m_{H_3^0}$ values) can be moderately coupled to W^+W^- when $m_{Z'}$ is small, even though this coupling vanishes asymptotically. Also worthy of note are the extrema of the $H_{Z'}^0 W^+ W^-$ coupling. This coupling actually changes sign as $m_{H^\pm}$ is varied at fixed $m_{H_3^0}$. In the allowed $m_{H^\pm}$ range it takes it maximum value when $m_{H^\pm}$ is at its minimum allowed value (where $m_{H_2^0}=0$), falls to 0 as $m_{H^\pm}$ (and also $m_{H_2^0}$) increases, and goes to its minimum value of the opposite sign as $m_{H^\pm}$ increases further towards its upper allowed value (and $m_{H_2^0}$ falls back to 0). When this coupling is maximum in absolute value, it can be a non-negligible fraction of SM strength, and $H_{Z'}^0 \to W^+W^-$ (and ZZ) will turn out to be the dominant decays. Further, even though its maximum values occur for $m_{H_2^0} \sim 0$, a restriction such as $m_{H_2^0} \geq 40$ GeV does not visibly affect the extreme values unless $m_{H_3^0}$ is fairly small. (This last statement also applies to $H^0_{\rm deg}$.)

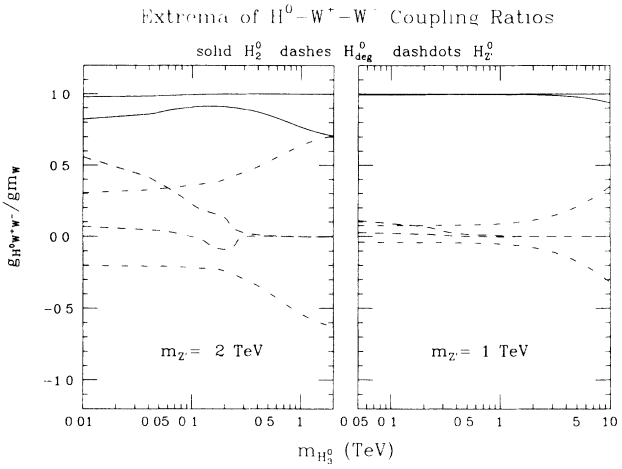

FIG. 5. Extrema of couplings of H_2^0, $H^0_{\rm deg}$, and $H_{Z'}^0$ to W^+W^- as a function of $m_{H_3^0}$ for $m_{Z'}=0.2$ TeV and $m_{Z'}=1$ TeV. We have normalized relative to the SM coupling of $g m_W$. Results for the ZZ couplings of these Higgs bosons are identical if normalized to $g m_{Z_{\rm SM}}/\cos\theta_W$.

Regarding the $Z'Z'$ channel, we see asymptotically that the only Higgs boson which couples significantly is the $H_{Z'}^0$. This remains true nonasymptotically, and this channel is never important in Higgs-boson decays since $m_{H_{Z'}^0} \approx m_{Z'}$ and $H_{Z'}^0 \to Z'Z'$ is never possible.

Finally, we mention that, on the theoretical side, it will be interesting to determine if any of the VV' scattering channels become strongly interacting if the Z' or H_3^0

masses are taken too large. Unlike the minimal supersymmetric model with no SU(2)×U(1)-singlet Higgs fields, we see from Eqs. (31)–(33) that vector-boson couplings to heavy Higgs bosons do not all vanish, and eventually tree-level unitarity will be violated.

V. HIGGS-BOSON PRODUCTION AT e^+e^- AND HADRON COLLIDERS

In the previous section we obtained the two types of couplings, quark-antiquark and vector-vector, that are responsible for the production of Higgs bosons. We now outline expectations for Higgs-boson production mechanisms using these results.

A. Higgs-boson production via quark-antiquark couplings

The quark-antiquark coupling of a neutral Higgs boson to a heavy quark determines one of its most important production processes at a hadron collider, namely gluon-gluon fusion to Higgs bosons via a heavy-quark triangle graph. Indeed, in the limit of large quark mass, the effective ggH coupling becomes independent of quark mass, since the $q\bar{q}$ coupling grows like m_q. From the results of the previous section we see that $H^0_{\rm deg}$, H^0_2, and H^0_3 are produced at full SM rate. All are dependent on the value of m_t, and cross sections are maximal when m_H is of order $2m_t$ (where the virtual t-quark triangle loop is at maximal strength). For a recent computation of such cross sections see Ref. 26. Analogously, $H^0_{Z'}$ production via gg fusion depends on the probably large exotic h-quark masses, and will not die away until $m_{H^0_{Z'}}$ is significantly beyond $2m_h$. In addition, h quarks of all three generations contribute, so that if the h quarks are all heavy, one gets a factor of 3 at amplitude level. However, the scale of the $H^0_{Z'}h\bar{h}$ coupling is set by $g_1/m_{Z'}$ (compared to g/m_W in the SM case), and the resulting gg fusion cross section will not be very large unless the Z' is quite light. To quote a specific example, suppose that there are three h quarks of mass 200 GeV, and that we take $m_{H^0_{Z'}}=0.4$ TeV. (The h mass choice corresponds to maximizing the gg fusion h-quark triangle graph for this choice of $m_{H^0_{Z'}}$.) Then the results of Ref. 26 may be rescaled to the coupling constant given in Eq. (21), and we find a cross section of 0.25 pb at the SSC.

The charged Higgs boson is produced at a hadron collider via the subprocess $g\bar{b}\to\bar{t}H^+$. This reaction turns out to have a remarkably large cross section.[26] Even for a charged-Higgs-boson mass of order 1 TeV, $\sigma\sim 1$ pb, corresponding to 10^4 events in a standard SSC year of $L=10^4\ {\rm pb}^{-1}$.

B. Higgs-boson production using vector bosons

Phenomenologically, Higgs-boson couplings to vector-boson pairs are crucial to three types of Higgs-boson production processes. These are production by vector-boson fusion, bremsstrahlung from a virtual vector boson, and Z' decays. In the SM, WW and ZZ fusion dominate Higgs-boson production once the Higgs-boson mass is $\gtrsim 0.3$ TeV. This is true at high energies for both hadron colliders and e^+e^- colliders. A second process which also makes use of $VV'H$ vertices, is virtual V^* production followed by $V^*\to V'H$; this is of particular importance at an e^+e^- collider with center of mass energy only moderately larger than the Higgs-boson mass of interest. Let us first focus on the fusion production reaction.

In the E_6 theory such processes could be of dramatically reduced importance. First, the H^0_2 which has the dominant couplings to WW and ZZ for large $m_{Z'}$ is also sufficiently light that its production is dominated by gg fusion at a hadron collider, with WW and ZZ fusion providing $\lesssim 20\%$ of the total (depending on the top-quark mass). Second, the W^+W^- and ZZ couplings to $H^0_{\rm deg}$ are only likely to be significant when both $m_{Z'}$ and $m_{H^0_3}$ are small (recall that small $m_{H^0_3}$ also implies small $m_{H^0_{\rm deg}}$) where, again, gg fusion will be dominant at a hadron collider. Third, since the $WWH^0_{Z'}$ coupling squared is always $\lesssim 0.1$ of SM strength, the WW fusion cross section for $H^0_{Z'}$ production is also of no practical importance. Combined with the small size of the gg fusion cross section discussed earlier, we see that the $H^0_{Z'}$ is very hard to produce, at both e^+e^- and hadron colliders. The importance of ZZ' fusion for $H^0_{\rm deg}$ production and of $Z'Z'$ fusion for $H^0_{Z'}$ production is critically dependent upon $m_{Z'}$. Computations of ZZ' and $Z'Z'$ fusion production processes were performed for the Superconducting Super Collider (SSC) in a different model in Ref. 27. Rescaling the couplings to those appropriate in the present case shows that only for $m_{H^0_{Z'}}\sim m_{Z'}$ below ~ 0.4 TeV will one find $H^0_{Z'}$ cross sections at the SSC above 0.1 pb, and that $m_{H^0_{Z'}}\sim m_{Z'}$ of order ~ 0.2 TeV is required for cross sections of order 1 pb. Similarly, the ZZ' fusion process for $H^0_{\rm deg}$ is only capable of yielding 1-pb-level cross sections for $m_{Z'}\lesssim 0.3$ TeV. Clearly, if $m_{Z'}\gtrsim 0.5$ TeV, these processes are not useful. At an e^+e^- collider, it is well known that the Z' is too weakly coupled to electrons for ZZ' or $Z'Z'$ fusion to be significant. In fact, even the ZZ fusion process for the SM Higgs boson is very small.[28]

Finally, we recall that the coupling of H^+ to W^+Z is proportional to the very small ZZ' mixing angle δ, while the H^0_3 has no VV couplings at all. As a result, vector-boson-fusion processes do not contribute to H^+ or H^0_3 production.

Production of Higgs bosons via bremsstrahlung from a virtual vector boson suffers much the same fate as do the fusion processes. For a heavy Z', only the H^0_2 will have a significant cross section coming from this source.

C. Higgs-boson production in Z' decays

As we have seen above, H^0_2 and $H^0_{\rm deg}$ both couple to ZZ'. This opens up the possibility of finding these two Higgs bosons as decay products of the Z' (Refs. 5, 9, 29, and 30). Also, the large $H^+Z'W^-$ coupling leads to H^+ production in Z' decays.[5] Thus we consider

$$Z'\to ZH^0_{2,\rm deg} \tag{37}$$

and

$$Z' \to W^{\mp} H^{\pm} . \tag{38}$$

We shall describe the results of Ref. 5, which employ the full mass-matrix diagonalization machinery. Among the possible decays the process $Z' \to H_2^0 Z$ is of greatest interest since it is almost always kinematically allowed, even for $m_{Z'}$ as low as 0.2 TeV.

In assessing the possibilities for Higgs-boson detection in the modes (37) and (38) we require the branching ratio for a generic $Z' \to HV$ decay. It can be easily expressed in terms of the $f_{HV} \equiv g_{Z'HV}/(g m_V)$, discussed earlier in Sec. IV B, as

$$B_{HV}^{Z'} = \frac{9 f_{HV}^2}{40 \tan^2\theta_W} K(m_{Z'}^2, m_H^2, m_V^2) B_{e^+e^-}^{Z'} , \tag{39}$$

where the kinematical factor is given by

$$K(a,b,c) = L^{3/2} + 12(c/a) L^{1/2} ,$$

with

$$L(a,b,c) = [(a+b-c)^2 - 4ab]/a^2 ,$$

and $B_{e^+e^-}^{Z'}$ is the branching ratio for $Z' \to e^+e^-$ decay. The value of $B_{e^+e^-}^{Z'}$ depends upon how many fermion-antifermion channels are open. Ignoring supersymmetric partner modes, it can vary from 0.036, if only standard model fermion decays are allowed, to 0.009, if three full families of E_6 fermion modes are allowed.[31] As stated earlier, asymptotically in $m_{Z'}$ we find (at $\tan\beta \sim 1$) that

$$f_{H_2^0 Z} \simeq \tfrac{3}{5} f_{H_{\rm deg}^0 Z} \simeq \tfrac{3}{5} f_{H^{\pm} W^{\mp}} \simeq \tfrac{1}{2} \tan\theta_W , \tag{40}$$

so that H_2^0, $H_{\rm deg}^0$, and $H^{\pm}$ are produced in Z' decays in the ratio 9:25:50 (the extra factor of 2 in the $H^{\pm}$ modes coming from the two different charge states). Nonasymptotically there is some variation of the f_{HV}'s but it is useful in the following discussions to refer to a "typical" case:

$$f_{HV} = 0.5, \quad K = 1, \quad B_{e^+e^-}^{Z'} = 0.009$$
$$\Longrightarrow B_{HV}^{Z'} = 1.8 \times 10^{-3} . \tag{41}$$

We also note that the Z or W, produced in association with a Higgs boson, might have to be detected in a leptonic decay mode in order to keep backgrounds under control. Keeping e and μ modes, the branching ratios for $Z \to l^+ l^-$ and $W \to l\nu$ are $B_{l^+l^-}^{Z} \sim 0.06$ and $B_{l\nu}^{W} \sim 0.16$, respectively. Altogether, we require $\gtrsim 10^5$ Z"s to have a detectable number of $Z' \to HV$ decays in the leptonic V decay channels, while only $\gtrsim 10^4$ Z"s would be required if the hadronic V decay channels can be employed.

In e^+e^- collisions the peak rate for Z' production (in the absence of beam energy smearing) is given in units of $\sigma_{\rm point} = (4\pi\alpha^2)/(3s)$ by

$$R_{\rm peak}^{Z'} = \frac{9 B_{e^+e^-}^{Z'}}{\alpha^2} . \tag{42}$$

For the parameters of Eq. (41) we obtain $R_{\rm peak}^{Z'} \approx 1327$ and $R_{\rm peak}^{Z'} B_{HV}^{Z'} \approx 2$. Assuming that a typical e^+e^- collider will achieve an integrated luminosity $\gtrsim 10^3/\sigma_{\rm point}$, we find a large number of events for discovery of several of the E_6 Higgs bosons in Z' decays, especially if some of the extra E_6 $f\bar{f}$ decay modes of the Z' are kinematically forbidden. Even if we must include $B_{l^+l^-}^{Z}$ or $B_{l\nu}^{W}$, we are left with hundreds of events. Of course, it could happen that $m_{H_3^0} \geq m_{Z'}$ and $m_{Z'} \gtrsim 0.5$ TeV, in which case the only kinematically allowed decay of Z' to a Higgs boson would be $Z' \to H_2^0 Z$. As discussed previously the $f_{H_2^0 Z}$ value is such that this decay would generally be observable.

Turning to the situation at the Superconducting Super Collider (SSC), the cross sections for Z' production have been summarized in Ref. 31. For small ZZ' mixing they vary from $\sim 2.2 \times 10^3$ pb at $m_{Z'} = 0.2$ TeV to ~ 22 pb at $m_{Z'} = 1$ TeV and ~ 1.7 pb at $m_{Z'} = 2$ TeV. The typical parameters (41) correspond to ~ 35 events, before including $B_{l^+l^-}^{Z}$ or $B_{l\nu}^{W}$, for every 2 pb of Z' cross section, at an integrated yearly luminosity of 10^4 pb^{-1}. At a hadron collider backgrounds will be severe unless we detect the Z or W in a leptonic decay mode. Thus we include $B_{l^+l^-}^{Z}$ or $B_{l\nu}^{W}$ and find that event rates at the SSC for an E_6 Higgs boson produced via Z' decays are only likely to be reasonable if $m_{Z'} \lesssim 1$ TeV, although searches at higher $m_{Z'}$ values might be possible if $B_{e^+e^-}^{Z'}$ is larger than 0.009.

The major backgrounds to Higgs-boson detection in Z' decays will depend upon the precise secondary decay modes of the Higgs boson produced. Typically, backgrounds are most difficult if the Higgs boson decays primarily to standard-model fermions, as will be the case for a light Higgs boson. A first consideration of the backgrounds in this case appears in Ref. 5, with the conclusion that they should not be a problem in e^+e^- collisions, but that they may be fairly severe at a hadron collider such as the SSC.

D. Comparison of e^+e^- and hadron colliders

Using the above results, we give a first-level comparison of the abilities of e^+e^- and hadron colliders to probe the E_6 Higgs sector.

1. e^+e^- collisions

(1) An e^+e^- collider remains the ideal choice for finding a light H_2^0, whether produced via vector-boson fusion, virtual vector bremsstrahlung, or in the decays of the new Z'.

(2) e^+e^- colliders are also ideal for finding a light $H_{\rm deg}^0$ or $H^{\pm}$ using the decays of the new Z', assuming, of course, that the Z' can be produced and that the decays are kinematically allowed.

(3) If $m_{Z'}$ and $m_{H_3^0}$ (which is $\sim m_{H_{\rm deg}^0}$) are small then $H_{\rm deg}^0$ can also have sizable W^+W^- and ZZ couplings. (The H_2^0 and $H_{\rm deg}^0$ share the SM coupling strength squared.) The $H_{\rm deg}^0$ production rate at an e^+e^- collider might be as large as 25% of that for an H_2^0 of similar mass, although it can also be quite small, depending upon

the precise λ value that is appropriate.

(4) If $s_{e^+e^-} > 4m^2_{H^\pm}$ then the charged Higgs boson are easily pair produced at an e^+e^- collider and backgrounds should not prevent studying them even if they decay primarily to SM heavy-quark channels.

(5) The $H^0_{Z'}$ is generally totally inaccessible at an e^+e^- collider, due to the smallness of its couplings to W^+W^- and ZZ. However, if the Z' turns out to be very light, the $H^0_{Z'}$ can be produced via $Z'^* \to Z'H^0_{Z'}$.

(6) Similarly the H^0_3 will normally be extremely difficult to produce in e^+e^- collisions due to the absence of any VV couplings. However, it may be possible to produce H^0_3 in association with either H^0_2 or $H^0_{\rm deg}$ in Z' decay if the corresponding decay is kinematically allowed. (The relevant couplings are discussed in Sec. VI A.)

(7) If the $H^\pm$ and $H^0_{\rm deg}$ cannot be found in Z' decays (either because $m_{H^\pm} \sim m_{H^0_{\rm deg}} \gtrsim m_{Z'}$ or because the Z' is too heavy to be produced), they too will be very difficult to produce at an e^+e^- collider—the $H^\pm$ has no couplings to $ZW^\pm$ and the $H^0_{\rm deg}VV$ couplings are likely to be strongly suppressed relative to SM-type strength (see Fig. 5).

(8) Generally speaking, any Higgs boson with significant production cross section will be observable even if it decays primarily to SM fermions, since backgrounds to such channels at an e^+e^- collider are relatively mild.

2. *Hadron collisions*

(1) A hadron collider will not have a significant gg fusion cross section to $H^0_{Z'}$ [via the h loop(s)], unless $m_{H^0_{Z'}}$ and, hence, $m_{Z'}$ is $\lesssim 0.4$ TeV. Since, its W^+W^- and ZZ couplings are quite small, these fusion processes will not be important. Finally, the $Z'Z'$ fusion process can only be significant when $m_{H^0_{Z'}} \sim m_{Z'} \lesssim 0.4$ TeV, where the gg fusion process would dominate in any case. Thus, if $m_{Z'}$ is heavy, the $H^0_{Z'}$ will not be easily produced, let alone detected at a hadron machine.

(2) The H^0_3, H^0_2, and $H^0_{\rm deg}$ cross sections from gg fusion should be of typical SM strength, and will be significant, depending upon the size of m_t relative to the Higgs-boson mass in question.

(3) VV fusion processes will not play a significant role in the production of $H^0_{\rm deg}$, since it decouples from W^+W^- and ZZ when it is sufficiently massive that VV fusion processes could have become important relative to gg fusion.

(4) H^0_3 does not couple to VV at the tree level so that only the gg fusion process is relevant for its production.

(5) The $H^\pm$ will be produced via processes of the type $g\bar{b} \to \bar{t}H^+$. The resulting cross section is comparable in strength to the gg fusion cross sections for H^0_3 and $H^0_{\rm deg}$ at the same mass.

(6) Unfortunately, even though the production cross sections are significant, Higgs bosons that decay primarily to heavy SM fermions will be difficult to detect at a hadron collider due to large QCD backgrounds. Only when the masses of $H^\pm$, H^0_3 and $H^0_{\rm deg}$ are small enough that the gg fusion cross sections are very large is there hope; in this instance rare decay modes of the Higgs boson appear to be usable.[32,33] However, as we show below, supersymmetric modes and other exotic modes characteristic of a complicated Higgs sector tend to be quite important in the decays of the heavy Higgs bosons, in which case a hadron machine could allow more complete access to the Higgs sector than an e^+e^- collider.

VI. HIGGS-BOSON COUPLINGS TO HV, HH, AND $\tilde{\chi}\tilde{\chi}$ CHANNELS

The Higgs-boson–quark–antiquark and Higgs-boson–vector–vector couplings, while dominant in considerations involving the production of the Higgs bosons, are not the only couplings of importance when it comes to the Higgs-boson decays. In this section we consider the remaining couplings that must be included in fully assessing the branching ratios of the E_6-model Higgs bosons to various different final states. There are three crucial sets of couplings which arise at tree level and yield two-body final states: (1) the couplings of Higgs bosons to other Higgs bosons plus a vector boson; (2) the trilinear self-couplings of the Higgs bosons, which allow decay of one Higgs boson to two others; (3) the couplings of the Higgs bosons to supersymmetric particle pairs. In considering these couplings we shall continue to make the approximation that we can neglect intergenerational couplings. As well as affecting the Higgs-boson-to-$\tilde{\chi}\tilde{\chi}$ decays, as discussed earlier, such intergenerational couplings could also result in such decays as Higgs boson to unhiggs boson plus vector boson, and Higgs boson to Higgs boson plus unhiggs boson, etc. By neglecting (in first approximation) intergenerational mixing, we are assuming that such decays have relatively small branching ratios.

As outlined earlier, which pairs of supersymmetric particles are allowed in the decay of a particular Higgs boson is model dependent. In the minimal supersymmetry model studies of Ref. 12 both squark/slepton pairs and neutralino/chargino pairs were studied, for several different mass scale possibilities. It was found that when both types of pair states were allowed, the neutralino/chargino pair states were dominant. In addition, it is likely that E_6 models prefer a rather large gluino mass and that the squarks and sleptons will be even more massive than the gluino. In Sec. III we demonstrated that even if $M_{\tilde{g}} \sim 0.5$ TeV there would still be many relatively light chargino and neutralino states, since their masses tended to be set by the scale of M and M', which are of order $M_{\tilde{g}}/4$ and $M_{\tilde{g}}/8$, or by $m_{Z'}$, which could be significantly smaller than $M_{\tilde{g}}$. Thus, in our study the only pairs of supersymmetric particles that we shall incorporate are those containing neutralinos and/or charginos, with masses computed for representative values of $M_{\tilde{g}}$ and $m_{Z'}$.

In the following three subsections we will give brief overviews of the three different types of couplings enumerated above. Details will be relegated to the Appendix.

A. *HHV* couplings

The *HHV* couplings are relatively easily given in terms of the eigenvectors $\mathbf{H}_\alpha$ introduced in Sec. IV A. The expressions appear in the Appendix along with our normalization conventions. All the formulas appearing there are exact in terms of the Higgs-boson eigenvectors; in the asymptotic domain the approximate eigenvector forms of Eq. (20) may be employed. It is useful to state the results that apply to this limit. We find

$$g_{W^-H^+H_2^0}\simeq 0,\quad g_{W^-H^+H_{Z'}^0}\simeq\frac{-g\rho}{2n}\ ,$$
$$g_{W^-H^+H_{\rm deg}^0}\simeq\frac{g}{2},\quad g_{W^-H^+H_3^0}\simeq\frac{-ig}{2}\ ; \tag{43}$$

$$g_{ZH^+H^-}\simeq-\frac{-g\cos2\theta_W}{2\cos\theta_W},\quad g_{ZH_3^0H_{\rm deg}^0}\simeq\frac{-ig}{2\cos\theta_W}\ ,$$
$$g_{ZH_3^0H_2^0}\simeq 0,\quad g_{ZH_3^0H_{Z'}^0}\simeq\frac{ig\rho}{2\cos\theta_W n}\ ; \tag{44}$$

$$g_{Z'H^+H^-}\simeq\frac{-g_1}{6}(1-5\cos^2\beta)\ ,$$
$$g_{Z'H_3^0H_{\rm deg}^0}\simeq\frac{-ig_1}{6}(1-5\cos^2\beta)\ ,$$
$$g_{Z'H_3^0H_2^0}\simeq\frac{5ig_1\sin2\beta}{12}\ , \tag{45}$$
$$g_{Z'H_3^0H_{Z'}^0}=O\left[\frac{\gamma}{n},\frac{\rho}{n}\right]\ .$$

Because of the many different couplings we will not plot nonasymptotic results, but most of the interesting features of these couplings and their implications for Higgs-boson decays can already be read off the asymptotic results. Note in particular the following points.

(1) Even though the $W^-H^+H_{Z'}^0$ and $ZH_3^0H_{Z'}^0$ couplings are ρ/n "suppressed," the $H_{Z'}^0$ decays to VH final states will turn out to be an important part of the $H_{Z'}^0$ total width when the $H_{Z'}^0$ is substantially heavier than H^+ and H_3^0. This is due to the presence of longitudinal V polarization states in these modes. (Of course, it is important to recall that the $H_{Z'}^0$ has quite weak couplings to W^+W^- and ZZ, and its decay widths to these competing channels will not necessarily be dominant.)

(2) Decays of the type $H_3^0\to Z'H_2^0$ are allowed when $m_{H_3^0}$ is large, and will be very important due to the longitudinal Z' modes and the full strength coupling. We also note that at small $m_{H_3^0}$, the $H_3^0\to ZH_2^0$ decay can be significant since the corresponding coupling is not negligible in that region.

(3) Despite large couplings of $H_{\rm deg}^0$ to W^-H^+ and ZH_3^0, these modes are never phase space allowed due to the near degeneracy of $H_{\rm deg}^0$ with H^+ and H_3^0.

(4) Of course, H_2^0 decays using the above couplings are never phase space allowed.

(5) Decays of the type $H^+\to W^+H_2^0$ and $H^+\to W^+H_{Z'}^0$ are suppressed due the very small couplings indicated in Eq. (43), combined with the presence of the competing channel (at high $m_{H^\pm}$) $H^+\to W^+Z'$ with large coupling, as discussed in Sec. IV B. Decays of the type $H^+\to W^+H_{\rm deg}^0$ and $H^+\to W^+H_3^0$ are absent, despite the large coupling indicated in Eq. (43), because of the near degeneracy in mass of H^+, $H_{\rm deg}^0$ and H_3^0.

(6) There are many HH modes for the decay of the Z' that couple with full strength. These can have a significant impact on the Z' width and detection.[34]

B. *HHH* couplings

We turn now to the *HHH* couplings. These are rather complicated but can be summarized in a relatively compact fashion using the eigenvectors defined in Eq. (20), as shown in the Appendix. However, not all such couplings are of potential importance in Higgs-boson decays. For instance, only at very small $m_{H_3^0}$ is there a possibility for H_2^0 to decay to two other Higgs bosons, namely, $H_3^0H_3^0$, and the relevant coupling is very small in that region. Similarly, since the H^+ and H_3^0 must always couple to themselves in the *HHH* couplings, they have no *HH* decays.

Thus, only couplings for $H_{Z'}^0$ and $H_{\rm deg}^0$ are of potential importance, and, in the latter case, only those to the possibly phase-space-allowed channels of $H_2^0H_2^0$, and (at large $m_{H_{\rm deg}^0}$) $H_{Z'}^0H_{Z'}^0$. As for other couplings, we shall give the large $m_{Z'}$, $m_{H_3^0}$ limits. The asymptotic limits can easily be obtained using the asymptotic forms of the $\mathbf{H}_\alpha$ given in Eq. (20) and are actually quite good approximations over a large region of $m_{H_3^0}$ so long as $m_{Z'}$ is not too small. Of course, our later numerical analysis of Higgs-boson branching ratios uses exact numerical results for the $\mathbf{H}_\alpha$ obtained from the Higgs-boson mass matrix diagonalization. Asymptotically, we find:

$$g_{H_{Z'}^0H_{\rm deg}^0H_2^0}\simeq\frac{1}{2\sqrt{2}}(\tfrac{5}{6}g_1^2n\sin2\beta+2\lambda A\cos2\beta)\ ,$$
$$g_{H_{Z'}^0H_2^0H_2^0}\simeq\frac{-1}{\sqrt{2}}[2\lambda^2n-\tfrac{5}{18}g_1^2n(1+3\sin^2\beta)-\lambda A\sin2\beta]\ ,$$
$$g_{H_{Z'}^0H_{\rm deg}^0H_{\rm deg}^0}\simeq 2g_{H_{Z'}^0H_3^0H_3^0}\simeq g_{H_{Z'}^0H^+H^-}$$
$$\simeq\frac{-1}{\sqrt{2}}[2\lambda^2n-\tfrac{5}{18}g_1^2n(1+3\cos^2\beta)+\lambda A\sin2\beta]\ , \tag{46}$$

$$g_{H_{\rm deg}^0H_{Z'}^0H_{Z'}^0}\simeq g_{H_{\rm deg}^0H_2^0H_2^0}\simeq\frac{-\lambda A}{\sqrt{2}n}(2\gamma\cos2\beta-\rho\sin2\beta)\ . \tag{47}$$

A brief survey is in order.

(1) The $H_{Z'}^0HH$ couplings can be quite large. In fact, the *HH* decay modes of the $H_{Z'}^0$ can be dominant. Let us comment on the $H_{Z'}^0$ couplings to $H_2^0H_2^0$, $H_3^0H_3^0$ and $H_{\rm deg}^0H_2^0$, for the case of $m_{Z'}=0.6$ TeV. (The $H_{Z'}^0H_{\rm deg}^0H_{\rm deg}^0$ and $H_{Z'}^0H^+H^-$ couplings are always roughly a factor 2 larger than the coupling for $H_{Z'}^0H_3^0H_3^0$.) These turn out to agree very well with the asymptotic formulas above,

once the appropriate λ values are substituted. All the couplings are potentially big, although the $H^0_{Z'}H^0_2H^0_2$ coupling changes sign (and hence must vanish at some point) as one varies $m_{H^\pm}$ (and hence λ) at fixed $m_{H^0_3}$; this is also true of the $H^0_{Z'}H^0_{\rm deg}H^0_{\rm deg}$, $H^0_{Z'}H^0_3H^0_3$, and $H^0_{Z'}H^+H^-$ couplings at small $m_{H^0_3}$. (For graphs of the behavior of the extrema of these couplings as a function of $m_{H^0_3}$ see Ref. 20.) Because of the low mass of the H^0_2, the kinematic inaccessibility of other HH modes, and the smallness of other classes of channels, it turns out that the $H^0_{Z'}\to H^0_2H^0_2$ decays can be dominant at large $m_{H^0_3}$. At small $m_{H^0_3}$ all the HH channels become phase space allowed and are significant. (The H^+H^- channel is a factor of 2 larger than $H^0_{\rm deg}H^0_{\rm deg}$ due to the identical particle factor suppression in the latter case, and a factor of 8 larger than the $H^0_3H^0_3$ channel which, in addition to being suppressed by the identical particle factor, has only $\frac{1}{4}$ the coupling strength squared.)

(2) Regarding the $H^0_{\rm deg}$, the asymptotic formulas suggest that its couplings to the possibly allowed channels of $H^0_2H^0_2$ and (at large $m_{H^0_{\rm deg}}\sim m_{H^0_3}$) $H^0_{Z'}H^0_{Z'}$ are quite small. This, indeed, turns out to be the case, except at very small $m_{H^0_3}$ where the $H^0_{\rm deg}\to H^0_2H^0_2$ modes can be significant.

C. $H\tilde{\chi}\tilde{\chi}$ couplings

Finally, we turn to the couplings of the Higgs bosons to the chargino and neutralino pair channels. These are determined in terms of the diagonalizing matrices discussed in Sec. III: U, V, and N. Explicit expressions and conventions are given in the Appendix. We note that, in general, there are both right- and left-handed couplings to consider. However, in the case of neutral-Higgs-boson couplings to $\tilde{\chi}^\pm\tilde{\chi}^\mp$ and $\tilde{\chi}^0\tilde{\chi}^0$ channels the left and right couplings have the same absolute magnitude, and can be easily obtained from one another using Eqs. (A15) and (A19) of the Appendix. There are, of course, a large number of couplings. However, it is quite straightforward to obtain asymptotic results for these couplings, and these are given in the Appendix. In fact, these "asymptotic" results may also be used nonasymptotically if one is careful to write these couplings usings the $\tilde{\chi}^0_{B'}\cdots\tilde{\chi}^0_{\tilde{N}_1-\tilde{B}_1}$ and $\tilde{\chi}^+_{\tilde{W}^+},\tilde{\chi}^+_{\tilde{H}^+}$ notation given earlier in Sec. III. Because, these states retain their identity to first approximation for all $m_{H^0_3}$, the asymptotic results appropriately reordered to correspond to mass-ordered eigenstates can be used to get a good idea of the coupling magnitudes at any point in the $\lambda, m_{H^0_3}$ space. This procedure is described in more detail in the Appendix.

Only a few general points regarding the Higgs-boson couplings to neutralino/chargino channels are worth noting here. First, the Appendix makes it clear that over much of parameter space there are actually relatively few important couplings, but that those that are significant will be of order λ, g or $g'=g_1$. In fact, for any Higgs-boson decay there is almost always one or more allowed neutralino/chargino decay channels with substantial coupling. Recalling that W^+W^- and ZZ channels are not important for our heavy Higgs bosons, and that only the $t\bar{t}$ (or, for the $H^0_{Z'}$, the $h\bar{h}$) channel will have coupling of order g, we find that the neutralino/chargino modes will be an extremely important component of Higgs-boson decays, and will almost always dominate SM fermion modes.

VII. HIGGS-BOSON DECAYS AND DETECTION

In order to fully examine the possibilities for detecting the E_6 model Higgs bosons, either in the inclusive production modes or through Z' decays, a full assessment of all the decay modes of each of the Higgs bosons is required. In particular, we have argued that in the case of the heavier Higgs bosons supersymmetric decay modes will be important, due to the substantial couplings and the relatively low mass scale of the neutralino/chargino sector. (As discussed earlier we will not include any squark or slepton decay modes in the computations that follow. Their masses are generally larger than the mass of the gluino which, in the scenario we investigate has a mass of 0.5 TeV. Thus, squark and slepton decay channels are likely to have a threshold substantially above that for the neutralinos and charginos. As discussed earlier, even when allowed they will not be as important as the neutralino/chargino channels at high Higgs-boson masses.) Also, modes in which a heavy-Higgs-boson decays to a pair of lighter Higgs bosons or to a vector boson in association with a lighter Higgs boson must be considered. In contrast, the decays of the light H^0_2 will be dominated by SM channels for moderate $M_{\tilde{g}}$ values. Of course, if a small $M_{\tilde{g}}$ scale is appropriate (e.g., $M_{\tilde{g}}\lesssim 200$ GeV), resulting in some very light neutralinos and charginos, H^0_2 decays to neutralinos and charginos could become important. However, one must be careful that the lightest chargino is not so light as to violate known experimental bounds, of order 30 GeV (Ref. 35). In this section we will give an overview of the branching ratios for Higgs-bosons decays to both standard-model channels and the above-mentioned more exotic channels. We shall consider the $m_{Z'}=0.6$ TeV case, and compute masses and mixings in the neutralino/chargino sector assuming $M_{\tilde{g}}=0.5$ TeV, the case considered earlier in discussing the neutralino/chargino masses. In a certain sense, this latter assumption may be a pessimistic one in that it leads to smaller branching ratios for these supersymmetric channels than would obtain for lighter $M_{\tilde{g}}$ values. We complete our parameter specification by taking $m_t=70$ GeV and $m_h=250$ GeV (for the third generation h—the first- and second-generation h's are assumed to be considerably lighter). This m_h value has been deliberately taken to be fairly small so that we can display the role of the $h\bar{h}$ mode in $H^0_{Z'}$ decays, should it be allowed.

We begin by noting that, with regard to decays, the results of Sec. IV B can be summarized as follows: whenever a VV' channel (with $V,V'=Z$ or $W^\pm$) is phase-space allowed for a given Higgs boson, the coupling of this Higgs boson to the VV' channel is very small. In addition, couplings to modes containing Z' are proportional

to g_1 and thus such modes naturally contribute less strongly than the low-mass vector-boson modes, even when phase-space allowed. Since it is primarily the longitudinal modes of VV' decay channels that can lead to a large Higgs-boson width, it is not surprising that all the Higgs bosons of this theory remain quite narrow. Only the H_3^0, $H_{\rm deg}^0$, and $H^{\pm}$ can become massive enough that VV' modes containing the Z', as well as modes containing a vector boson and a lighter Higgs boson, become important and total widths begin to become significant. Thus, for the $m_{Z'}=0.6$ TeV, $M_{\tilde g}=0.5$ TeV case that we are focusing on, H_2^0 always remains very narrow, $H_{Z'}^0$ has $\Gamma \lesssim 15$ GeV at $m_{H_3^0}=3$ TeV (recall that this is our basic parameter) while H_3^0, $H^{\pm}$, and $H_{\rm deg}^0$ (all approximately degenerate in mass) have $\Gamma \lesssim 100$ GeV at $m_{H_3^0}=3$ TeV. The behavior of the widths as a function of $m_{H_3^0}$ is illustrated in Fig. 6, where we plot the maximum and minimum widths of all the Higgs bosons in the usual fashion. The delayed growth in the Higgs-boson widths is, of course, closely related to the fact that the Higgs sector of this theory does not become strongly interacting, and bad high-energy behavior of various scattering amplitudes involving scalar modes does not emerge, until very high energy scales.

With this background, it is not surprising that non-SM modes could play a major role in the decays of these Higgs bosons over this region of $m_{H_3^0}$ parameter space. In particular, the neutralino/chargino channels provide a significant fraction of the total decays of the heavier Higgs bosons. To emphasize this point, we plot the maximum and minimum branching ratios for the sum over all $\tilde\chi\tilde\chi$ modes for each of the different Higgs bosons in Fig. 7. For this figure we have taken a very light gluino mass, $M_{\tilde g}=0.2$ TeV and have required that $m_{H_2^0}$ be ≥ 40 GeV. We see that, once phase-space allowed, it is not uncommon for the $\tilde\chi\tilde\chi$ modes to have a net branching ratio of order 50%, especially at large $m_{H_3^0}\sim m_{H_{\rm deg}^0}\sim m_{H^{\pm}}$. (We note that $H_{Z'}^0$ does not have substantial branching ratio to $\tilde\chi\tilde\chi$ at high $m_{H_3^0}$ since it couples primarily to the heavier $\tilde\chi\tilde\chi$ states which generally have combined mass larger than $m_{H_{Z'}^0}\sim m_{Z'}$.) Note also that if $M_{\tilde g}$ is as small as 200 GeV, many of the neutralinos and charginos, in particular $\tilde\chi_{\tilde B}^0$, $\tilde\chi_{\tilde W_3}^0$, and $\tilde\chi_{\tilde W}^{+}$, can become light enough that these decay modes can have substantial importance in H_3^0, $H_{\rm deg}^0$, and $H^{\pm}$ decays at low Higgs-boson masses. They even become a substantial component of H_2^0 decays when the H_2^0 takes on the maximum mass allowed at the higher $m_{H_3^0}$ values plotted. Were we to plot results for the same $M_{\tilde g}$ value, but with $m_{H_2^0}\geq 40$ GeV not required, we would find that the $\tilde\chi\tilde\chi$ decays of all the Higgs bosons, except the $H_{Z'}^0$, are enhanced, relative to those appearing in Fig. 7, at low $m_{H_3^0}$. The reason is that the lower bounds on the $\tilde\chi$ masses are decreased substantially once the lower bound on λ is decreased by removing the lower bound on $m_{H_2^0}$. The $H_{Z'}^0$ is an exception since at low $m_{H_3^0}$ it remains massive, unlike the other Higgs bosons.

Let us now turn to a more general survey of all of the channels of importance in the decays of the various Higgs

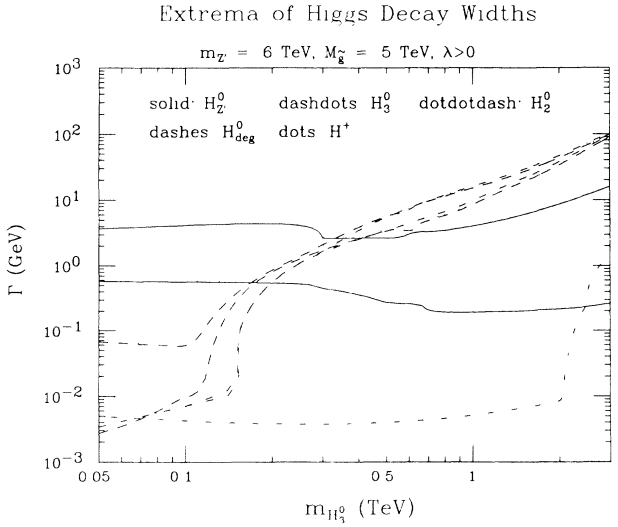

FIG. 6. We plot the total decay widths of all the Higgs bosons as a function of $m_{H_3^0}$. The maximum and minimum values are given as found when scanning over all allowed λ (or $m_{H^{\pm}}$) values at a given $m_{H_3^0}$. We have chosen $M_{\tilde g}=0.5$ TeV and $m_{Z'}=0.6$ TeV, and taken $\tan\beta=1.1$. Squark and slepton channels are not included.

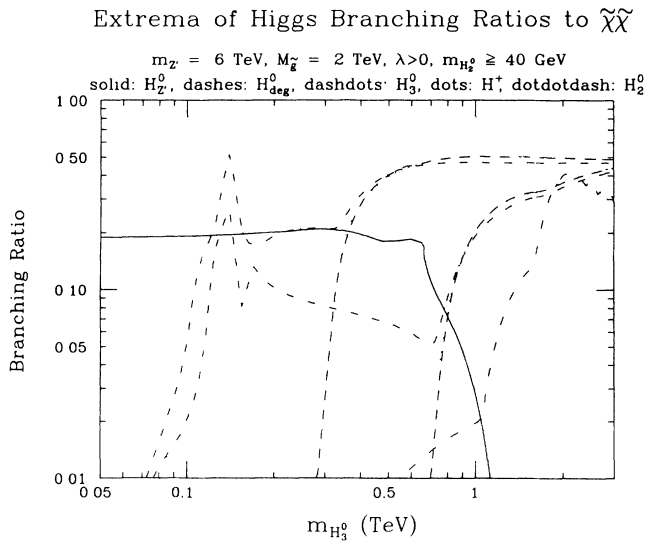

FIG. 7. Branching ratios for the $H_{Z'}^0$, $H_{\rm deg}^0$, H_3^0, $H^{\pm}$, and H_2^0 to decay to all $\tilde\chi\tilde\chi$ channels. The $H_{Z'}^0$ branching ratios are sensitive to the h-quark masses; we have taken the third-generation h-quark mass to be 250 GeV and assumed those belonging to the first and second generations are much lighter and can be neglected in the $H_{Z'}^0$ decays because of their weaker coupling. We take $M_{\tilde g}=0.2$ TeV, $\lambda>0$ and plot branching-ratio extrema for $\tilde\chi\tilde\chi$ channels in the case where we require $m_{H_2^0}\geq 40$ GeV. Note that the minimum branching ratio for $H_{Z'}^0$ is off the scale of the graph. We have taken $m_{Z'}=0.6$ TeV and $\tan\beta=1.1$.

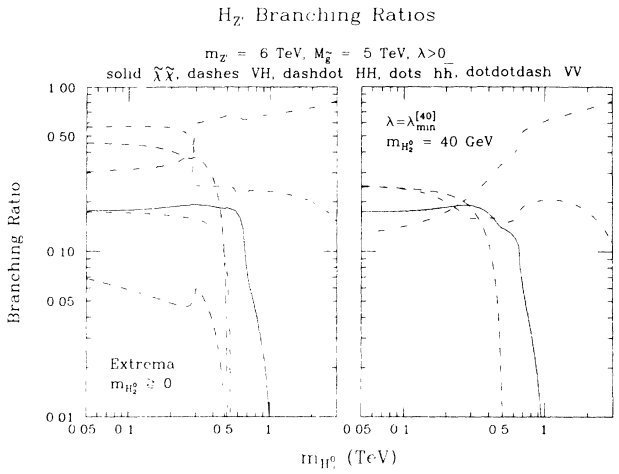

FIG. 8. We present branching ratios for $H_{Z'}^0 \to \tilde{\chi}\tilde{\chi}$, HH, VH, VV, and $h\bar{h}$. We sum over all allowed channels of a given type for the first four mode classes. We include only the third-generation h quark as described in the caption to Fig. 7. There are two plots. In the first, we present the maxima and minima for a given mode, with no $m_{H_2^0}$ lower limit. In the second we present the branching ratio for each mode at $\lambda_{min}^{[40]}$, defined as the minimum value of λ that yields $m_{H_2^0}=40$ GeV. For both plots $M_{\tilde{g}}=0.5$ TeV, $m_{Z'}=0.6$ TeV, and $\tan\beta=1.1$.

bosons. For this survey we shall adopt the moderate $M_{\tilde{g}}=0.5$ TeV, $m_{Z'}=0.6$ TeV values considered in several previous graphs, including those of the neutralino/chargino masses, Figs. 3 and 4. We shall also take $\tan\beta=1.1$ and $\lambda>0$. We present graphs for $H_{Z'}^0$, H_3^0, H_{deg}^0, and H^+, in Figs. 8–11, respectively, which display branching ratios for all general classes of modes that are important in the decays of the given Higgs boson. Two different types of plots are presented. In the first, we give the extrema of the important branching ratios with no lower limit imposed on the H_2^0 mass. In the second we plot branching ratios computed at a unique λ value at each $m_{H_3^0}$. This unique value is $\lambda_{min}^{[40]}$, the minimum $\lambda>0$ value that yields $m_{H_2^0}\geq 40$ GeV. (In fact, at $\lambda=\lambda_{min}^{[40]}, m_{H_2^0}$ is exactly 40 GeV.) The easiest plots to absorb are those of the latter type which have a unique branching ratio for a given channel at each $m_{H_3^0}$ value. It it easily seen that the combined branching ratios for the various modes yield close to 100% of a given Higgs-boson decay. We note that for the choice of $M_{\tilde{g}}=0.5$ TeV that we have made, the H_2^0 decays are entirely similar to those of a standard-model Higgs boson of the same mass. For additional graphs of branching ratios at different $m_{Z'}$ and $M_{\tilde{g}}$ values, and for the $\lambda<0$ choice at the same values of $m_{Z'}$ and $M_{\tilde{g}}$ considered here, see Ref. 20. The graphs presented here turn out to be quite representative.

We may now survey the prospects for Higgs-boson decays and detection.

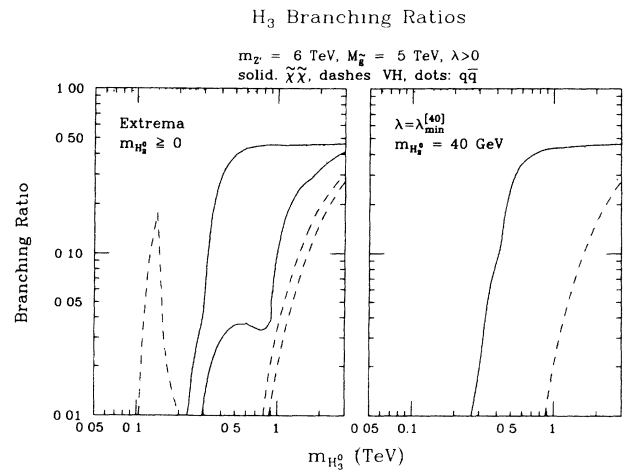

FIG. 9. Similar to Fig. 8, but for H_3^0: $\tilde{\chi}\tilde{\chi}$, $q\bar{q}$, and VH channels are important.

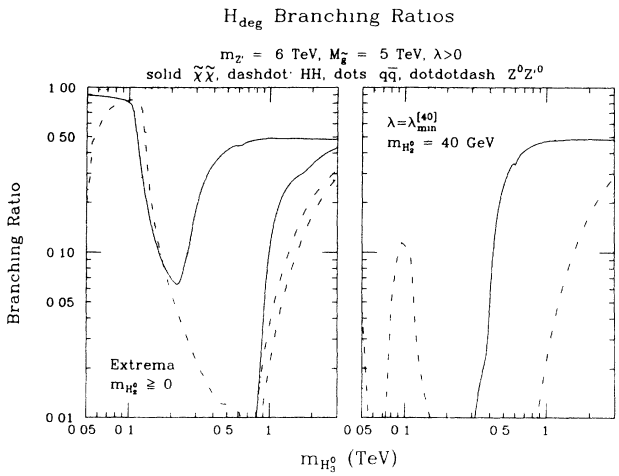

FIG. 10. Similar to Fig. 8, but for H_{deg}^0: $\tilde{\chi}\tilde{\chi}$, $q\bar{q}$, ZZ', and HH channels are important.

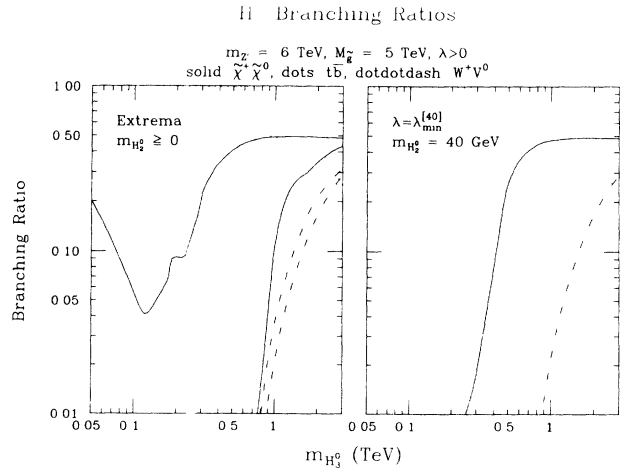

FIG. 11. We present the same types of plots as in Fig. 8, but for the H^+ decays to the $\tilde{\chi}\tilde{\chi}$, W^+V^0 (this is dominantly W^+Z'), and $t\bar{b}$ channels; VH channels are never important. Parameter choices are the same as for Fig. 8.

(1) H_2^0: We remark that the H_2^0 decays entirely to light-SM-fermion channels until $m_{H_3^0} \gtrsim 3$ TeV [beyond the range allowed by the imprecise bounds mentioned earlier—see Eq. (13) and the discussion which follows], at which point it can become massive enough (for λ appropriately chosen) to decay, as well, to $t\bar{t}$, WW, and ZZ modes. Of course, we have already seen in Fig. 7 that if the neutralinos and charginos are light (i.e., $M_{\tilde{g}}$ is small), then $\tilde{\chi}\tilde{\chi}$ decays will become important at the higher $m_{H_2^0}$ values.

(2) $H_{Z'}^0$: The decays of this Higgs boson exhibit considerable complexity. At high $m_{H_3^0}$ (not linked to $m_{H_{Z'}^0} \sim m_{Z'}$) the $\tilde{\chi}\tilde{\chi}$ modes are small as mentioned earlier, whereas VV (WW and ZZ are in the ratio 2:1) and HH (entirely $H_2^0 H_2^0$ once $m_{H_3^0}$ is large enough that the other Higgs bosons become heavy) may be either large or very small depending upon the precise value of λ. The VV and $H_2^0 H_2^0$ channels are maximal when λ is such that $m_{H_2^0}$ is near 0. (Recall that the relevant couplings change sign as λ varies from its minimum to its maximum value at fixed $m_{H_3^0}$.) When they are not substantial, the $h\bar{h}$ modes dominate and signatures for the h-quark decays should be very distinctive.[36] At lower $m_{H_3^0}$ values, a full battery of modes appears. Aside from the still important VV, HH, and $h\bar{h}$ modes these include $\tilde{\chi}\tilde{\chi}$ modes and VH modes [ZH_3^0 and $W^{\pm}H^{\mp}$ are in the ratio 1:2 given by state counting, see Eqs. (43) and (44)]. (Both of the VV and all, except $H_{\rm deg}^0 H_2^0$, of the HH modes vanish somewhere as λ varies between its minimum and maximum value, though not all at the same point.) Of course, if $m_{H_{Z'}^0}$ is small (due to a small Z' mass) many of the above modes might not be allowed: for instance, the $h\bar{h}$ decays will probably not be allowed, and probably the $\tilde{\chi}\tilde{\chi}$ modes with significant coupling would also be kinematically forbidden. Despite the many possible modes with good signatures, the $H_{Z'}^0$ may still be very difficult to find, due to its small production cross sections. At a hadron collier the gg fusion cross section will be substantially smaller than that for a SM Higgs boson, even if the h quark has large mass. At an e^+e^- machine, it will also be very difficult to produce the $H_{Z'}^0$ due to the absence of couplings to W^+W^- and ZZ, as found in Sec. IV B. Detection is not likely unless the Z' (and, correspondingly, the $H_{Z'}^0$) mass is small, in which case the $Z'Z'$ fusion could become significant, and the $H_{Z'}^0 h\bar{h}$ coupling ($\sim \frac{5}{6} g_1 m_h / m_{Z'}$) is not as suppressed so that gg fusion could be important at a hadron machine. For more details on cross sections, refer to Secs. V A and V B.

(3) H_3^0: Neutralino/chargino modes tend to be important except for small values of $m_{H_3^0}$, where (at least for $M_{\tilde{g}} = 0.5$ TeV) they become kinematically forbidden. (A lower bound on $m_{H_2^0}$ increases the region over which they are phase-space disallowed.) At high $m_{H_3^0}$, a variety of modes are important as can be seen from the asymptotic couplings for H_3^0 to $\tilde{\chi}\tilde{\chi}$ states given in the Appendix. Of course, $t\bar{t}$ and other SM heavy-fermion channels play a significant role at low $m_{H_3^0}$, but decrease in importance as $m_{H_3^0}$ passes ~ 1 TeV and the $\tilde{\chi}\tilde{\chi}$ modes become dominant. At low $m_{H_3^0}$ there is also a peak in the VH mode coming from the ZH_2^0 channel; asymptotically, however, this coupling becomes very small. Its place is taken in the high-$m_{H_3^0}$ region by the $Z'H_2^0$ mode, which becomes increasingly significant. If the neutralino/chargino modes are dominant, the H_3^0 should be detectable at the SSC out to about 0.5 TeV after which its gg fusion cross section becomes too small. At small $m_{H_3^0}$ it may be necessary to employ rare decay modes (e.g., the $\gamma\gamma$ mode[33]) when the SM-fermion decays are dominant. In contrast with these expectations for the SSC, cross sections at an e^+e^- collider are almost certainly too small to allow detection.

(4) $H_{\rm deg}^0$: There are many similarities to H_3^0. Neutralino/chargino modes tend to be important for most $m_{H_3^0}$ values. However, this region of importance extends even to small $m_{H_3^0}$, provided there is no lower bound imposed on the $\tilde{\chi}$ masses through a lower bound on λ or $m_{H_2^0}$, since the $H_{\rm deg}^0$ never has mass less than ~ 80 GeV and there is always phase space for the lighter $\tilde{\chi}\tilde{\chi}$ modes. In fact, it is the light $\tilde{\chi}^0\tilde{\chi}^0$ states that can be important at low $m_{H_3^0}$, while at large $m_{H_{\rm deg}^0} \sim m_{H_3^0}$, heavier $\tilde{\chi}^0\tilde{\chi}^0$ states as well as $\tilde{\chi}_1^{\pm}\tilde{\chi}_2^{\mp}$ states become important. The ZZ' mode becomes significant at high $m_{H_{\rm deg}^0}$; it can be as large as ~ 0.3 of the total at $m_{H_{\rm deg}^0} \sim 3$ TeV. The $t\bar{t}$ mode tends to be dominant (if allowed) for small $m_{H_3^0}$ decreasing slowly as the $\tilde{\chi}\tilde{\chi}$ modes turn on at high $m_{H_3^0}$. Finally, the $H_2^0 H_2^0$ mode becomes very strong for $m_{H_3^0} \lesssim 0.14$ TeV, where the $t\bar{t}$ mode becomes phase-space forbidden. VH modes are never important since the H's to which $H_{\rm deg}^0$ couples are more or less degenerate with the $H_{\rm deg}^0$ itself. Conclusions are similar to those for the H_3^0: the gg fusion mode cross section is possibly sufficient for detection of the $H_{\rm deg}^0$ at the SSC out to $m_{H_{\rm deg}^0} \sim 0.5$ TeV; when important the $\tilde{\chi}\tilde{\chi}$ modes are the most useful; however, it may be necessary to employ rare decay modes (in particular the $\gamma\gamma$ mode[33]) when SM fermion decay modes are dominant at small $m_{H_3^0}$.

(5) H^+: For low masses it is clear that H^+ decays primarily to $t\bar{b}$ making detection very difficult except at an e^+e^- collider. As $m_{H^{\pm}}$ passes ~ 0.3 TeV the $\tilde{\chi}^+\tilde{\chi}^0$ modes can become up to 50% of the decays and may allow detection of the H^+ at a hadron collider as well as at an e^+e^- collider; further study is required to be more definite. Finally, we note the increasing importance of VV modes (dominated by W^+Z') in H^+ decays as $m_{H^{\pm}} \sim m_{H_3^0}$ becomes large. These would have a clean signature at a hadron collider if at least one of the V's decayed leptonically, but the associated event rate would be very low, due to the $\lesssim 0.05$ pb cross section at the SSC

(Ref. 26) for $m_{H^\pm} \gtrsim 2$ TeV, where the VV modes become significant. Overall, detection at an e^+e^- collider is probably only limited by the phase space for H^+H^- pair production while at a hadron collider it is limited by the region of $m_{H^\pm}$ over which the $gb \to H^-t$ and $g\bar{b} \to H^+\bar{t}$ cross section is substantial. (At the SSC, the latter cross sections are of reasonable size, i.e, $\gtrsim 1$ pb, out to about $m_{H^\pm} \sim 0.8$ TeV.)

The challenge for the heavy Higgs boson is obvious. We must fully explore the final states which arise from the above myriad of possible decays. For all the heavy Higgs bosons we must note that many of their decay products—e.g., neutralinos, charginos, Z,Z', and other Higgs bosons—will in turn decay. The resulting final states are clearly very complex and backgrounds must be carefully explored. This task will be difficult and will require detailed Monte Carlo calculations work on the part of our experimental colleagues.

VIII. CONCLUSIONS

We have investigated the Higgs-boson and neutralino/chargino mass spectra of the simplest E_6-based grand unification model, and explored implications for the production and detection of the Higgs bosons. The highly constrained nature of the model implies that predictions need only be explored as a function of a few parameters. In this paper we have chosen these parameters to be (1) the mass of the Z'; (2) the ratio of Higgs-doublet vacuum expectation values, $\tan\beta = v_2/v_1$; (3) the mass of the pseudoscalar Higgs boson, $m_{H_3^0}$; (4) the value of the supersymmetric coupling parameter λ; and (5) the gluino mass $M_{\tilde{g}}$. As discussed in Ref. 5, the new e^+e^- colliders are likely to place constraints on Z-Z' mixing that, combined with the strong theoretical preference for $v_2 > v_1$, will imply that the Z' mass must be $\gtrsim 0.5$ TeV. In addition, the model becomes somewhat unnatural if $m_{Z'} > 1$ TeV. Thus we have largely focused on the representative value of $m_{Z'} = 0.6$ TeV. For such a moderate Z' mass the same probable future e^+e^- constraints are likely to constrain (in the context of this model) $\tan\beta$ to be near 1; we have chosen $\tan\beta = 1.1$ for most of our analysis. Results for larger values of $\tan\beta$ are not very different so long as $\tan\beta \lesssim 3$. Regarding the gluino mass, we have focused on a representative value of $M_{\tilde{g}} = 0.5$ TeV, typical of the values appropriate for this model. Again, a value of $M_{\tilde{g}}$ that is much larger than 1 TeV would be unnatural in the context of the theory.

The remaining two parameters are those most fundamentally connected to the Higgs sector. We showed in Sec. II how the Higgs spectrum is essentially completely determined by a choice for $m_{H_3^0}$. At each $m_{H_3^0}$ only a narrow range of λ values and, consequently, other Higgs-boson masses are possible. Particularly interesting is the lightest Higgs scalar boson, the H_2^0, whose mass is bounded from above and could be extremely light. In addition, there is the $H_{Z'}^0$ Higgs scalar which is always approximately degenerate with the Z', the charged Higgs bosons $H^\pm$, and the remaining scalar Higgs boson $H_{\rm deg}^0$, which are approximately degenerate in mass and have $m_{H_{\rm deg}^0} \sim m_{H^\pm} \sim m_{H_3^0}$, except at small $m_{H_3^0}$. Various theoretical constraints suggest strongly that $m_{H_3^0} \lesssim 1$ TeV. Since the neutralino/chargino sector is an important component of Higgs-boson decays, we also investigated the mass spectrum of this sector as a function $m_{H_3^0}$ (no parameters beyond those mentioned already are required) and found masses that were highly correlated with the Higgs-boson and Z' masses.

We then proceeded to investigate the production of all the Higgs bosons. Since H_2^0, $H_{\rm deg}^0$, $H^\pm$, and H_3^0 all have fermion couplings very similar to those that would be appropriate to a standard-model Higgs boson, these will be copiously produced via gg fusion (or $gb \to tH^\pm$) at a hadron collider up to masses of the order of 0.5 TeV (assuming $m_t \lesssim 100$ GeV). The $H_{Z'}^0$ couples only to the exotic h quarks of the model, and this coupling is small unless the Z' is quite light. It is likely to have a very marginal gg fusion cross section. Turning to the VV couplings of the Higgs bosons, we found that only the light H_2^0 has substantial couplings to WW and ZZ. Thus, the other Higgs bosons cannot be easily produced using standard-model mechanisms that rely on these couplings. In particular, the VV fusion mechanism at both e^+e^- and hadron colliders is never important, and high mass Higgs bosons will be very inaccessible. Also absent (except for the H_2^0) is the bremsstrahlung mechanism of $V^* \to V + H$, which is very useful for a SM Higgs boson at an e^+e^- collider.

However, the existence of the Z' does open up the possibility of an important new source of Higgs-boson production: namely, production of a large number of Z''s followed by $Z' \to H_2^0 Z$, $H_{\rm deg}^0 Z$, or $H^\pm W^\pm$. The associated couplings are generally substantial, and the Z' decays could potentially reveal important information regarding the Higgs sector of the underlying E_6-breaking scheme. Backgrounds to searching for such decays will be least severe at an e^+e^- machine. However, if large numbers of Z''s are not available, or if a given Higgs boson has mass higher than Z', then we would have to rely on the standard production modes just discussed. We have seen that this presents a problem for producing the Higgs bosons other than the H_2^0 at an e^+e^- collider. (Of course, $H^\pm$ can be pair produced if light enough.)

Returning to hadron colliders, we found that the fusion mechanisms, $gg \to H_3^0, H_{\rm deg}^0, H_2^0$ and $gb \to tH^\pm$, yield substantial cross sections up to moderate Higgs-boson masses. However, if these Higgs bosons coupled only to SM heavy-fermion channels, there would clearly be no possibility of discovering them at the SSC, except at very low masses where production rates are high enough that rare decay modes might be useful. Fortunately, at moderate and larger masses, various exotic decay modes become important and are often dominant, especially supersymmetric modes involving neutralinos and charginos. Such decay channels were explored in detail in Sec. VII.

At either an e^+e^- or hadron collider, the importance of supersymmetric decay modes for all Higgs bosons oth-

er than the H_2^0 implies that the search for Higgs bosons at future colliders may well become a branch of supersymmetric phenomenology. Other evidence for supersymmetry may already be available, although, if squarks and gluinos should turn out to be very heavy, it is certainly possible that supersymmetric decay products of the Higgs bosons may be the first direct evidence for supersymmetry. At a minimum, information on the Higgs-boson sector will provide extremely useful consistency checks and will be crucial to pinning down the details of the underlying supersymmetric theory. A careful evaluation of Higgs-boson detection possibilities in the plethora of exotic modes awaits further work, but we are cautiously optimistic for those situations where adequate production rate is available. Unless an e^+e^- collider has sufficient energy and luminosity to produce a large number of Z''s *and* the Higgs bosons other than the H_2^0 are light enough to be produced in its decays, it is likely that a hadron collider will provide more complete access to the full Higgs spectrum of an E_6-based model.

ACKNOWLEDGMENT

This work was supported in part by the Department of Energy.

APPENDIX: HIGGS-BOSON COUPLINGS TO HV, HH, AND $\tilde{\chi}\tilde{\chi}$

1. HHV couplings

Let us first enumerate the HHV couplings. These may be obtained from the $SSVV$ (S represents a scalar field and V a vector field) portion of the Lagrangian. One expands H_1, H_2, and N_1 in terms of the vacuum expectation values v_1, v_2, and n, plus physical mass eigenstates fields. The exact results may be easily summarized. Our couplings (denoted by $g_{VH'H}$) are defined with all particles in-going, as the coefficient of $(p-p')\cdot\epsilon_V$ where p is the (incoming) momentum of H and p' is the (incoming) momentum of H'. We first give couplings involving a charged W. We find

$$g_{W^\mp H^\pm H_\alpha}=\frac{\pm g}{2}[\cos\beta H_\alpha(2)-\sin\beta H_\alpha(1)]\ , \qquad \alpha=2,\text{deg},Z'\ , \tag{A1}$$

$$g_{W^\mp H^\pm H_3^0}=\frac{-ig}{2}[\cos\beta H_3(2)+\sin\beta H_3(1)]\ .$$

Turning to the couplings to a neutral Z or Z', we first note that CP forbids all couplings other than ZH^+H^- and $ZH_3^0H_\alpha$ ($\alpha=2,\text{deg},Z'$), where $Z=Z$ or Z'. The mixing of the neutral gauge bosons leads to slightly more complicated formulas than in the W case. We find

$$g_{ZH^+H^-}=\frac{-g}{2}\left[\frac{-\cos\delta\cos2\theta_W}{\cos\theta_W}+\frac{\tan\theta_W\sin\delta}{3}(1-5\cos^2\beta)\right]\ ,$$

$$g_{ZH_3^0H_\alpha}=\frac{-ig}{2\cos\theta_W}\left[\frac{\sin\theta_W\sin\delta}{3}[5H_3(3)H_\alpha(3)-4H_3(2)H_\alpha(2)-H_3(1)H_\alpha(1)]-\cos\delta[H_3(1)\mathbf{H}_\alpha(1)-H_3(2)\mathbf{H}_\alpha(2)]\right]\ , \tag{A2}$$

where α runs over 2,deg,Z'; the Z' couplings are obtained by the replacements $-\cos\delta\to\sin\delta$ and $\sin\delta\to\cos\delta$. In the above, the $\mathbf{H}_\alpha$ are the eigenvectors defined in Sec. IV A. Note in particular that the exact expression for $H_3(i)$ ($i=1,2,3$) is given in Eq. (20).

2. HHH couplings

We turn now to the HHH couplings. These are rather complicated, but can be summarized in a relatively compact fashion using the eigenvectors defined in Eq. (A20). We first introduce the notation

$$\Pi_{\alpha\beta\gamma}(i,j,k)=\sum_{\{i,j,k\}\ \text{perms}} H_\alpha(i)H_\beta(j)H_\gamma(k)\ , \tag{A3}$$

for $\alpha,\beta,\gamma=2,\text{deg},Z'$, where i,j,k can take on the values 1,2,3, and the summation runs over all inequivalent permutations of fixed i,j,k values. That is, the sum consists of six terms if i,j,k are distinct, three terms if two of the three i,j,k indices are equal, and one term if $i=j=k$. For example, $\pi_{\alpha\alpha\alpha}(1,1,2)=3H_\alpha^2(1)H_\alpha(2)$ after summing over three terms. We then find that the Feynman rule couplings for three neutral scalars take the form

$$g_{H_\alpha H_\beta H_\gamma}=\frac{-1}{2\sqrt{2}}[\ \tfrac{25}{3}g_1^2 n\,\Pi_{\alpha\beta\gamma}(3,3,3)+(3g^2v_2+\tfrac{16}{3}g_1^2v_2+3g'^2v_2)\Pi_{\alpha\beta\gamma}(2,2,2)$$
$$+(3g^2v_1+\tfrac{1}{3}g_1^2v_1+3g'^2v_1)\Pi_{\alpha\beta\gamma}(1,1,1)+(4\lambda^2v_2-\tfrac{20}{9}g_1^2v_2)\Pi_{\alpha\beta\gamma}(3,3,2)$$
$$+(4\lambda^2v_1-\tfrac{5}{9}g_1^2v_1)\Pi_{\alpha\beta\gamma}(3,3,1)+(4\lambda^2n-\tfrac{20}{9}g_1^2n)\Pi_{\alpha\beta\gamma}(2,2,3)$$
$$+(-2\lambda A)\Pi_{\alpha\beta\gamma}(3,2,1)+(4\lambda^2n-\tfrac{5}{9}g_1^2n)\Pi_{\alpha\beta\gamma}(1,1,3)$$
$$+(-g^2v_1+4\lambda^2v_1+\tfrac{4}{9}g_1^2v_1-g'^2v_1)\Pi_{\alpha\beta\gamma}(2,2,1)$$
$$+(-g^2v_2+4\lambda^2v_2+\tfrac{4}{9}g_1^2v_2-g'^2v_2)\Pi_{\alpha\beta\gamma}(1,1,2)]\ , \tag{A4}$$

where α, β, and γ can take on any of the values 2,deg,Z'. The couplings involving the H_3^0 and $H^\pm$ are somewhat different. First, parity forbids all but $H_3^0H_3^0H_\alpha$ and $H^+H^-H_\alpha$ ($\alpha=2$,deg,Z') couplings. Second the structure of the allowed couplings is somewhat different. For the H_3^0 couplings we define

$$\Pi_{33\alpha}(i,j,k)=H_3(i)H_3(j)H_\alpha(k) \tag{A5}$$

and obtain

$$g_{H_3^0H_3^0H_\alpha}=\frac{-1}{2\sqrt{2}}\{\ \tfrac{25}{9}g_1^2n\,\Pi_{33\alpha}(3,3,3)+(g^2v_2+\tfrac{16}{9}g_1^2v_2+g'^2v_2)\Pi_{33\alpha}(2,2,2)$$
$$+(g^2v_1+\tfrac{1}{9}g_1^2v_1+g'^2v_1)\Pi_{33\alpha}(1,1,1)+(4\lambda^2v_2-\tfrac{20}{9}g_1^2v_2)\Pi_{33\alpha}(3,3,2)$$
$$+(4\lambda^2v_1-\tfrac{5}{9}g_1^2v_1)\Pi_{33\alpha}(3,3,1)+(4\lambda^2n-\tfrac{20}{9}g_1^2n)\Pi_{33\alpha}(2,2,3)$$
$$+(4\lambda A)[\Pi_{33\alpha}(3,2,1)+\Pi_{33\alpha}(2,1,3)+\Pi_{33\alpha}(3,1,2)]+(4\lambda^2n-\tfrac{5}{9}g_1^2n)\Pi_{33\alpha}(1,1,3)$$
$$+(-g^2v_1+4\lambda^2v_1+\tfrac{4}{9}g_1^2v_1-g'^2v_1)\Pi_{33\alpha}(2,2,1)$$
$$+(-g^2v_2+4\lambda^2v_2+\tfrac{4}{9}g_1^2v_2-g'^2v_2)\Pi_{33\alpha}(1,1,2)\}\ , \tag{A6}$$

where α can take on any of the values 2,deg,Z'. Finally, for the $H^\pm$ couplings it is convenient to introduce the two-component eigenvector

$$\mathbf{H}_+=\mathbf{H}_-\equiv\begin{bmatrix}\sin\beta\\ \cos\beta\end{bmatrix}\ , \tag{A7}$$

in terms of which we define

$$\Pi_{+-\alpha}(i,j,k)=H_+(i)H_-(j)H_\alpha(k)\ , \tag{A8}$$

where i,j run over 1,2 and k can take on the values 1,2,3. For the couplings involving $H^\pm$ we find

$$g_{H^+H^-H_\alpha}=\frac{-1}{2\sqrt{2}}\{\ (g^2v_2+\tfrac{16}{9}g_1^2v_2+g'^2v_2)\Pi_{+-\alpha}(2,2,2)+(g^2v_1+\tfrac{1}{9}g_1^2v_1+g'^2v_1)\Pi_{+-\alpha}(1,1,1)$$
$$+(4\lambda^2n-\tfrac{20}{9}g_1^2n)\Pi_{+-\alpha}(2,2,3)+(2\lambda A)[\Pi_{+-\alpha}(1,2,3)+\Pi_{+-\alpha}(2,1,3)]$$
$$+(4\lambda^2n-\tfrac{5}{9}g_1^2n)\Pi_{+-\alpha}(1,1,3)+(g^2v_1+\tfrac{4}{9}g_1^2v_1-g'^2v_1)\Pi_{+-\alpha}(2,2,1)$$
$$+(g^2v_2+\tfrac{4}{9}g_1^2v_2-g'^2v_2)\Pi_{+-\alpha}(1,1,2)+(g^2v_1-2\lambda^2v_1)[\Pi_{+-\alpha}(2,1,2)+\Pi_{+-\alpha}(1,2,2)]$$
$$+(g^2v_2-2\lambda^2v_2)[\Pi_{+-\alpha}(2,1,1)+\Pi_{+-\alpha}(1,2,1)]\}\ , \tag{A9}$$

where α can take on any of the values 2,deg,Z'. By substituting the asymptotic forms for the $\mathbf{H}_\alpha$'s given in Eq. (A20), we obtain the results given in the text. Our numerical analysis of the Higgs branching ratios uses exact results for the $\mathbf{H}_\alpha$.

3. $H\tilde{\chi}\tilde{\chi}$ couplings

The couplings of the Higgs bosons to the chargino and neutralino pair channels are determined in terms of the diagonalizing matrices discussed in Sec. III, U, V, and N. It is not too difficult to state the results for all the relevant couplings. First, for the charged-Higgs-boson couplings to a neutralino/chargino pair we have

$$g_{\bar{\tilde{\chi}}_i^0 \tilde{\chi}_j^+ H^-} = Q_{ij}'^L P_L + Q_{ij}'^R P_R \ , \tag{A10}$$

where $P_{L,R} = (1 \mp \gamma_5)/2$, $i = 1-6$, $j = 1,2$,

$$Q_{ij}'^L = -g \cos\beta N_{i5}^* V_{j1}^* + \lambda \sin\beta N_{i6}^* V_{j2}^* + \sqrt{2}\cos\beta V_{j2}^* \left(-\tfrac{2}{3} N_{i3}^* g_1 - \tfrac{1}{2} N_{i2}^* g' - \tfrac{1}{2} N_{i1}^* g\right) , \tag{A11}$$

and

$$Q_{ij}'^R = -g \sin\beta N_{i4} U_{j1} + \lambda \cos\beta N_{i6} U_{j2} + \sqrt{2}\sin\beta U_{j2} \left(-\tfrac{1}{6} N_{i3} g_1 + \tfrac{1}{2} N_{i2} g' + \tfrac{1}{2} N_{i1} g\right) . \tag{A12}$$

For the coupling of neutral Higgs bosons to chargino pairs we obtain

$$g_{\bar{\tilde{\chi}}_i^- \tilde{\chi}_j^+ H_\alpha} = Q_{ij}^L P_L + Q_{ij}^R P_R \ , \tag{A13}$$

where i,j take on the values 1,2 and $\alpha = 2,\text{deg},Z',3$. The Q matrices are given by

$$Q_{ij}^L = \eta_\alpha \frac{g}{\sqrt{2}} \left[V_{j2}^* U_{i1}^* H_\alpha(2) + V_{j1}^* U_{i2}^* H_\alpha(1) \right] + \eta_\alpha' \frac{\lambda}{\sqrt{2}} U_{i2}^* V_{j2}^* H_\alpha(3) \ , \tag{A14}$$

$$Q_{ij}^R = (Q_{ji}^L)^* \ , \tag{A15}$$

and η and η' are defined by

$$\eta_\alpha = \begin{cases} +i, & \alpha = 3 \ , \\ -1, & \alpha = 2,\text{deg},Z' \ , \end{cases} \qquad \eta_\alpha' = \begin{cases} +i, & \alpha = 3 \ , \\ +1, & \alpha = 2,\text{deg},Z' \ . \end{cases} \tag{A16}$$

Finally, for the coupling of neutral Higgs bosons to neutralino pairs we obtain Feynman-diagram level couplings:

$$g_{\bar{\tilde{\chi}}_i^0 \tilde{\chi}_j^0 H_\alpha} = Q_{ij}''^L P_L + Q_{ij}''^R P_R \ , \tag{A17}$$

where i,j take on the values 1–6, and $\alpha = 2,\text{deg},Z',3$. Of course, the neutralinos are Majorana particles and only $i \geq j$ need to be considered. The Q'' matrices are given by

$$\begin{aligned} Q_{ij}''^L = \{ & \eta_\alpha [(\tfrac{1}{6} N_{i4}^* N_{j3}^* g_1 - \tfrac{1}{2} N_{i4}^* N_{j2}^* g' + \tfrac{1}{2} N_{i4}^* N_{j1}^* g) H_\alpha(1) \\ & + (\tfrac{2}{3} N_{i5}^* N_{j3}^* g_1 + \tfrac{1}{2} N_{i5}^* N_{j2}^* g' - \tfrac{1}{2} N_{i5}^* N_{j1}^* g) H_\alpha(2) - \tfrac{5}{6} N_{j6}^* N_{j3}^* g_1 H_\alpha(3)] \\ & + \eta_\alpha' \frac{\lambda}{\sqrt{2}} [N_{i6}^* N_{j5}^* H_\alpha(1) + N_{i6}^* N_{j4}^* H_\alpha(2) + N_{i4}^* N_{j5}^* H_\alpha(3)] \} + \{ i \leftrightarrow j \} \end{aligned} \tag{A18}$$

and

$$Q_{ij}''^R = (Q_{ji}''^L)^* \ , \tag{A19}$$

with η and η' defined as in Eq. (A16).

It is, of course, again possible to obtain asymptotic expressions for all the above couplings. For this purpose we need only combine the asymptotic results for the $\mathbf{H}_\alpha$'s from Eq. (A20) with asymptotic results for the neutralino and chargino diagonalizing matrices, N, and U,V. We give below the leading asymptotic terms in these three matrices obtained in the approximation where

$$g v_1, g v_2, g' v_1, g' v_2 \ll \lambda n \ , \tag{A20}$$

$$N \simeq \begin{bmatrix} 0 & 1 & 0 & 0 & 0 & 0 \\ 1 & 0 & 0 & 0 & 0 & 0 \\ 0 & 0 & \frac{i}{\sqrt{2}} & 0 & 0 & \frac{i}{\sqrt{2}} \\ 0 & 0 & \frac{1}{\sqrt{2}} & 0 & 0 & \frac{-1}{\sqrt{2}} \\ 0 & 0 & 0 & \frac{i}{\sqrt{2}} & \frac{-i}{\sqrt{2}} & 0 \\ 0 & 0 & 0 & \frac{1}{\sqrt{2}} & \frac{1}{\sqrt{2}} & 0 \end{bmatrix} , \qquad U \simeq V \simeq \begin{bmatrix} 1 & 0 \\ 0 & i \end{bmatrix} . \tag{A21}$$

The columns for U and V appear in the order $\tilde{W}^{\pm},\tilde{H}^{\mp}$, while those for N are in the order $\tilde{W}_3,\tilde{B}',\tilde{B}_1,\tilde{H}_1,\tilde{H}_2,\tilde{N}_1$. The rows are ordered according to increasing eigenstate mass at large $m_{H_3^0}$. This ordering is appropriate once $m_{H_3^0}$ is beyond the region where level crossing occurs (see Figs. 3 and 4). However, these same forms for N, U, and V are also approximately valid at lower $m_{H_3^0}$ if one is careful to (1) imagine labeling the rows according to eigenstate composition; or (2) reorder the rows according to the mass ordering (of the various eigenstates) appropriate to the given $m_{H_3^0}$ value. An examination of this matrix quickly reveals the eigenstate basis discussed in the text. In particular, we see the identifications:

$$\begin{aligned}
&\tilde{\chi}_1^0\equiv\tilde{\chi}_{\tilde{B}'}^0,\quad \tilde{\chi}_4^0\equiv\tilde{\chi}_{\tilde{N}_1-\tilde{B}_1}^0,\quad \tilde{\chi}_1^{\pm}\equiv\tilde{\chi}_{\tilde{W}^+}^{+},\\
&\tilde{\chi}_2^0\equiv\tilde{\chi}_{\tilde{W}_3}^0,\quad \tilde{\chi}_5^0\equiv\tilde{\chi}_{\tilde{H}_1-\tilde{H}_2}^0,\quad \tilde{\chi}_2^{\pm}\equiv\tilde{\chi}_{\tilde{H}^+}^{+},\\
&\tilde{\chi}_3^0\equiv\tilde{\chi}_{\tilde{N}_1+\tilde{B}_1}^0,\quad \tilde{\chi}_6^0\equiv\tilde{\chi}_{\tilde{H}_1+\tilde{H}_2}^0,
\end{aligned}\tag{A22}$$

at large $m_{H_3^0}$. We stress again, however, that if we use the latter eigenstate notation the N, and U,V matrices remain approximately the same nonasymptotically, and the eigenbasis states retain their identity, to first approximation, for all $m_{H_3^0}$, as discussed in Sec. III, so long as Eq. (A20) is true. [For instance, at $m_{Z'}=0.6$ TeV, $n\sim 1.42$ TeV, and $m_{H_3^0}<240$ GeV is required before the minimum value of λ is such that $gv_1>\lambda n$. In fact, imposing $m_{H_2^0}\geq 40$, we find that $\lambda_{\min}^{[40]}$ is large enough that Eq. (A20) is true for all $m_{H_3^0}$ at this value of $m_{Z'}$.] As discussed previously, which of the eigenbasis states corresponds to a given $\tilde{\chi}_i$ mass-ordered eigenstate depends upon where in λ and $m_{H_3^0}$ parameter space one is looking.

Using the above matrix forms we may compute the neutralino and chargino couplings to the Higgs bosons. The following results are not only very accurate asymptotically, but also provide good approximations for all $m_{H_3^0}$ to the extent discussed above. Couplings not given below are small, becoming ~ 0 in the asymptotic limit. We employ the notations $c_\beta\equiv\cos\beta$ and $s_\beta\equiv\sin\beta$. We shall use the asymptotic mass eigenstate labeling; the reader must use the translation table of Eq. (A22) nonasymptotically. Asymptotically, we find for the neutral Higgs bosons the following left-handed couplings, Q_{ij}^L or $Q_{ij}^{\prime\prime L}$. Right-handed couplings are obtained by the operators (A15) and (A19).

(1) H_2^0:

$$\begin{aligned}
&\tilde{\chi}_1^-\tilde{\chi}_2^+:\ \frac{igs_\beta}{\sqrt{2}},\\
&\tilde{\chi}_2^-\tilde{\chi}_1^+:\ \frac{igc_\beta}{\sqrt{2}},\\
&\bar{\tilde{\chi}}_3^0\tilde{\chi}_5^0:\ -\left[\frac{\lambda}{2\sqrt{2}}(c_\beta-s_\beta)-\frac{g_1}{12}(c_\beta-4s_\beta)\right],\\
&\bar{\tilde{\chi}}_1^0\tilde{\chi}_5^0:\ \frac{-ig'}{2\sqrt{2}}(c_\beta+s_\beta),\\
&\bar{\tilde{\chi}}_3^0\tilde{\chi}_6^0:\ i\left[\frac{\lambda}{2\sqrt{2}}(c_\beta+s_\beta)+\frac{g_1}{12}(c_\beta+4s_\beta)\right],\\
&\bar{\tilde{\chi}}_1^0\tilde{\chi}_6^0:\ \frac{g'}{2\sqrt{2}}(c_\beta-s_\beta),\\
&\bar{\tilde{\chi}}_4^0\tilde{\chi}_5^0:\ i\left[\frac{\lambda}{2\sqrt{2}}(c_\beta-s_\beta)+\frac{g_1}{12}(c_\beta-4s_\beta)\right],\\
&\bar{\tilde{\chi}}_2^0\tilde{\chi}_5^0:\ \frac{ig}{2\sqrt{2}}(c_\beta+s_\beta),\\
&\bar{\tilde{\chi}}_4^0\tilde{\chi}_6^0:\ \left[\frac{\lambda}{2\sqrt{2}}(c_\beta+s_\beta)-\frac{g_1}{12}(c_\beta+4s_\beta)\right],\\
&\bar{\tilde{\chi}}_2^0\tilde{\chi}_6^0:\ \frac{-g}{2\sqrt{2}}(c_\beta-s_\beta).
\end{aligned}\tag{A23}$$

(2) H_{deg}^0:

$$\begin{aligned}
&\tilde{\chi}_1^-\tilde{\chi}_2^+:\ \frac{igc_\beta}{\sqrt{2}},\\
&\tilde{\chi}_2^-\tilde{\chi}_1^+:\ \frac{-igs_\beta}{\sqrt{2}},\\
&\bar{\tilde{\chi}}_3^0\tilde{\chi}_5^0:\ \left[\frac{\lambda}{2\sqrt{2}}(c_\beta+s_\beta)-\frac{g_1}{12}(4c_\beta+s_\beta)\right],\\
&\bar{\tilde{\chi}}_1^0\tilde{\chi}_5^0:\ \frac{-ig'}{2\sqrt{2}}(c_\beta-s_\beta),\\
&\bar{\tilde{\chi}}_3^0\tilde{\chi}_6^0:\ i\left[\frac{\lambda}{2\sqrt{2}}(c_\beta-s_\beta)+\frac{g_1}{12}(4c_\beta-s_\beta)\right],\\
&\bar{\tilde{\chi}}_1^0\tilde{\chi}_6^0:\ \frac{-g'}{2\sqrt{2}}(c_\beta+s_\beta),\\
&\bar{\tilde{\chi}}_4^0\tilde{\chi}_5^0:\ -i\left[\frac{\lambda}{2\sqrt{2}}(c_\beta+s_\beta)+\frac{g_1}{12}(4c_\beta+s_\beta)\right],\\
&\bar{\tilde{\chi}}_2^0\tilde{\chi}_5^0:\ \frac{ig}{2\sqrt{2}}(c_\beta-s_\beta),\\
&\bar{\tilde{\chi}}_4^0\tilde{\chi}_6^0:\ \left[\frac{\lambda}{2\sqrt{2}}(c_\beta-s_\beta)-\frac{g_1}{12}(4c_\beta-s_\beta)\right],\\
&\bar{\tilde{\chi}}_2^0\tilde{\chi}_6^0:\ \frac{g}{2\sqrt{2}}(c_\beta+s_\beta).
\end{aligned}\tag{A24}$$

(3) $H_{Z'}^0$:

$$\begin{aligned}
&\tilde{\chi}_2^-\tilde{\chi}_2^+:\ -\frac{\lambda}{\sqrt{2}},\\
&\bar{\tilde{\chi}}_3^0\tilde{\chi}_3^0,\bar{\tilde{\chi}}_4^0\tilde{\chi}_4^0:\ -\tfrac{5}{6}g_1,\\
&\bar{\tilde{\chi}}_5^0\tilde{\chi}_5^0,\bar{\tilde{\chi}}_6^0\tilde{\chi}_6^0:\ -\frac{\lambda}{\sqrt{2}}.
\end{aligned}\tag{A25}$$

(4) H_3^0:

$$\begin{aligned}
&\tilde{\chi}_1^- \tilde{\chi}_2^+ : \ \frac{gc_\beta}{\sqrt{2}} , \\
&\tilde{\chi}_2^- \tilde{\chi}_1^+ : \ \frac{gs_\beta}{\sqrt{2}} , \\
&\bar{\tilde{\chi}}_3^0 \tilde{\chi}_5^0 : \ i\left[\frac{\lambda}{2\sqrt{2}}(c_\beta - s_\beta) + \frac{g_1}{12}(4c_\beta - s_\beta)\right] , \\
&\bar{\tilde{\chi}}_1^0 \tilde{\chi}_5^0 : \ \frac{-g'}{2\sqrt{2}}(c_\beta + s_\beta) , \\
&\bar{\tilde{\chi}}_3^0 \tilde{\chi}_6^0 : \ -\left[\frac{\lambda}{2\sqrt{2}}(c_\beta + s_\beta) - \frac{g_1}{12}(4c_\beta + s_\beta)\right] , \\
&\bar{\tilde{\chi}}_1^0 \tilde{\chi}_6^0 : \ \frac{ig'}{2\sqrt{2}}(c_\beta - s_\beta) , \\
&\bar{\tilde{\chi}}_4^0 \tilde{\chi}_5^0 : \ \left[\frac{\lambda}{2\sqrt{2}}(c_\beta - s_\beta) - \frac{g_1}{12}(4c_\beta - s_\beta)\right] , \\
&\bar{\tilde{\chi}}_2^0 \tilde{\chi}_5^0 : \ \frac{g}{2\sqrt{2}}(c_\beta + s_\beta) , \\
&\bar{\tilde{\chi}}_4^0 \tilde{\chi}_6^0 : \ i\left[\frac{\lambda}{2\sqrt{2}}(c_\beta + s_\beta) + \frac{g_1}{12}(4c_\beta + s_\beta)\right] , \\
&\bar{\tilde{\chi}}_2^0 \tilde{\chi}_6^0 : \ \frac{ig}{2\sqrt{2}}(c_\beta - s_\beta) .
\end{aligned} \tag{A26}$$

Note that the $H^0_{\rm deg}$ and H_3^0 couplings can be simply obtained from those given for H_2^0: (a) for the $H^0_{\rm deg}$ we take the H_2^0 couplings and perform the operation $[c_\beta \to -s_\beta, s_\beta \to c_\beta]$; (b) for the H_3^0 couplings we begin with the H_2^0 couplings and perform the substitutions $[c_\beta \to s_\beta, s_\beta \to c_\beta, \lambda \to -\lambda]$ and multiply all couplings by an overall $-i$.

For the charged Higgs boson, the left- and right-handed couplings are not trivially related. We quote asymptotically results for both $Q_{ij}^{\prime L}$ and $Q_{ij}^{\prime R}$.

(1) Left-handed H^+ couplings:

$$\begin{aligned}
&\bar{\tilde{\chi}}_1^0 \tilde{\chi}_2^+ : \ \frac{ig' c_\beta}{\sqrt{2}} , \\
&\bar{\tilde{\chi}}_2^0 \tilde{\chi}_2^+ : \ \frac{igc_\beta}{\sqrt{2}} , \\
&\bar{\tilde{\chi}}_3^0 \tilde{\chi}_2^+ : \ -\frac{\lambda s_\beta}{\sqrt{2}} + \frac{2}{3} g_1 c_\beta , \\
&\bar{\tilde{\chi}}_4^0 \tilde{\chi}_2^+ : \ i\left[\frac{\lambda s_\beta}{\sqrt{2}} + \tfrac{2}{3} g_1 c_\beta\right] , \\
&\bar{\tilde{\chi}}_5^0 \tilde{\chi}_1^+ : \ \frac{-igc_\beta}{\sqrt{2}} , \\
&\bar{\tilde{\chi}}_6^0 \tilde{\chi}_1^+ : \ \frac{-gc_\beta}{\sqrt{2}} .
\end{aligned} \tag{A27}$$

(2) Right-handed H^+ couplings:

$$\begin{aligned}
&\bar{\tilde{\chi}}_1^0 \tilde{\chi}_2^+ : \ \frac{ig' s_\beta}{\sqrt{2}} , \\
&\bar{\tilde{\chi}}_2^0 \tilde{\chi}_2^+ : \ \frac{igs_\beta}{\sqrt{2}} , \\
&\bar{\tilde{\chi}}_3^0 \tilde{\chi}_2^+ : \ -\frac{\lambda c_\beta}{\sqrt{2}} + \tfrac{1}{6} g_1 c_\beta , \\
&\bar{\tilde{\chi}}_4^0 \tilde{\chi}_2^+ : \ -i\left[\frac{\lambda c_\beta}{\sqrt{2}} + \tfrac{1}{6} g_1 c_\beta\right] , \\
&\bar{\tilde{\chi}}_5^0 \tilde{\chi}_1^+ : \ \frac{-igs_\beta}{\sqrt{2}} , \\
&\bar{\tilde{\chi}}_6^0 \tilde{\chi}_1^+ : \ \frac{-gs_\beta}{\sqrt{2}} .
\end{aligned} \tag{A28}$$

This completes the discussion of the $H\tilde{\chi}\tilde{\chi}$ couplings.

*On leave of absence from Warsaw University, Warsaw, Poland.

[1] E. Witten, Phys. Lett. **155B**, 151 (1985); Nucl. Phys. **B258**, 75 (1985); P. Candelas, G. T. Horowitz, A. Strominger, and E. Witten, *ibid.* **B258**, 46 (1985).

[2] P. Binetruy, S. Dawson, I. Hinchliffe, and M. Sher, Nucl. Phys. **B273**, 501 (1986).

[3] J. Ellis, K. Enqvist, D. V. Nanopoulos, and F. Zwirner, Nucl. Phys. **B276**, 14 (1986).

[4] L. E. Ibanez and J. Mas, Nucl. Phys. **B286**, 107 (1987).

[5] J. F. Gunion, H. E. Haber, and L. Roszkowski, Phys. Lett. B **189**, 409 (1987).

[6] H. E. Haber and M. Sher, Phys. Rev. D **35**, 2206 (1987).

[7] J. Ellis, D. V. Nanopoulos, S. T. Petcov, and F. Zwirner, Nucl. Phys. **B283**, 93 (1987).

[8] M. Drees, Phys. Rev. D **35**, 2910 (1987).

[9] H. Baer, D. Dicus, M. Drees, and X. Tata, Phys. Rev. D **36**, 1363 (1987).

[10] J.-P. Derendinger, L. E. Ibanez, and H. P. Nilles, Nucl. Phys. **B267**, 365 (1986).

[11] J. F. Gunion and H. E. Haber, Nucl. Phys. **B272**, 1 (1986).

[12] J. F. Gunion and H. E. Haber, Nucl. Phys. **B278**, 449 (1986).

[13] S. Komamiya, in *Proceedings of the 1985 International Symposium on Lepton and Photon Interactions at High Energies*, Kyoto, Japan, 1985, edited by M. Konuma and K. Takahashi (Research Institute for Fundamental Physics, Kyoto University, 1986).

[14] B. Campbell, J. Ellis, M. K. Gaillard, D. V. Nanopoulos, K. A. Olive, Phys. Lett. B **180**, 77 (1986).

[15] L. W. Durkin and P. Langacker, Phys. Lett. **166B**, 436 (1986).

[16] V. Barger, N. G. Deshpande, and K. Whisnant, Phys. Rev. Lett. **56**, 30 (1986).

[17] P. J. Franzini and F. J. Gilman, Phys. Rev. D **35**, 855 (1987).

[18] H. P. Nilles, Phys. Rep. **110**, 1 (1984).

[19] J. Ellis, P. Franzini, and F. Zwirner, Phys. Lett. B **202**, 417 (1988).

[20] L. Roszkowski, Ph.D. thesis, University of California, Davis, 1987.

[21] W. Bartel *et al.*, Z. Phys. C **29**, 505 (1985); H. J. Behrend, *et al.*, *ibid.* **35**, 181 (1987).

[22] H. Baer, K. Hagiwara, and X. Tata, Phys. Rev. D **35**, 1598

(1987).
[23]E. Cohen, J. Ellis, K. Enqvist, J. S. Hagelin, D. V. Nanopoulos, and K. Olive, Phys. Lett. B **173**, 270 (1986).
[24]J. Ellis, J. S. Hagelin, D. V. Nanopoulos, K. Olive, and M. Srednicki, Nucl. Phys. **B238**, 453 (1984); G. Girardi and P. Salati, *ibid.* **B264**, 621 (1986).
[25]L. Roszkowski, in Proceedings of the 1987 Cargèse Summer School (unpublished).
[26]J. F. Gunion, H. E. Haber, F. E. Paige, Wu-Ki Tung, and S. S. D. Willenbrock, Nucl. Phys. **B294**, 621 (1987).
[27]J. F. Gunion, B. Kayser, R. N. Mohapatra, N. G. Deshpande, J. Grifols, A. Mendez, F. Olness, and P. B. Pal, in *Proceedings of the Summer Study on the Physics of the Superconducting Super Collider,* Snowmass, Colorado, 1986, edited by R. Donaldson and J. Marx (Division of Particles and Fields of the APS, New York, 1987), p. 197.
[28]See, for instance, J. F. Gunion, and A. Tofighi-Niaki, Phys. Rev. D **36**, 2671 (1987).
[29]S. Nandi, Phys. Lett. B **181**, 375 (1986).
[30]C. Dib and F. J. Gilman, Phys. Rev. D **36**, 1337 (1987).
[31]H. Haber, in *Supercollider Physics,* edited by D. E. Soper (World Scientific, Singapore, 1986), p. 194.
[32]See, for example, the review by J. F. Gunion *et al.*, Phys. Rev. D **34**, 101 (1986).
[33]J. F. Gunion, G. Kane, and J. Wudka, Nucl. Phys. **B299**, 231 (1988).
[34]V. Barger and K. Whisnant, Int. J. Mod. Phys. **A2**, 1327 (1987).
[35]See, for example, the limits found by the DESY PETRA group (Ref. 21) and those inferred using additional theoretical arguments in (Ref. 22).
[36]See, for example, the survey given by V. Barger, N. G. Deshpande, and J. F. Gunion, in *Proceedings of the Summer Study on the Physics of the Superconducting Super Collider* (Ref. 27).